October 2017

Regulation of Katanin Activity on Microtubules

Madison A. Tyler
University of Massachusetts Amherst

REGULATION OF KATANIN ACTIVITY ON MICROTUBULES

A Thesis Presented

by

MADISON A. TYLER

Submitted to the Graduate School of the
University of Massachusetts Amherst in partial fulfillment
of the requirements for the degree of

MASTER OF SCIENCE

SEPTEMBER 2017

Molecular and Cellular Biology

REGULATION OF KATANIN ACTIVITY ON MICROTUBULES

A Thesis Presented

by

MADISON A. TYLER

Approved as to style and content by:

_____
Jennifer L. Ross, Chair

_____
Peter Chien, Member

_____
Thomas Maresca, Member

_____
Dominique Alfandari, Director
Molecular and Cellular Biology

ACKNOWLEDGEMENTS

Thank you to my labmates who also supported me throughout this journey. I am lucky to call you my colleagues, as well as my friends. Thank you to Greg Petrucci Jr. for your many sacrifices and to Eliza Frechette for being my best cheerleader. I am grateful to my family, especially my mom, who knows me better than I know myself and who gives me strength, daily. I would like to especially thank Dr. Jennifer Ross for the opportunity to work under her guidance in this collaborative and highly interdisciplinary lab. Jenny, I am truly lucky to have had you as an advisor. I appreciate all the support and mentoring you have given me this year. Thank you opening my horizon and showing me that graduate school was an option. Thank you to my committee members, Dr. Peter Chien and Dr. Tom Maresca, for insightful conversation and helping me grow as a scientist and as an individual. Finally, thank you to Dr. Ned Debold for initially introducing the undergraduate me to Biophysics, a discipline I will forever love.

ABSTRACT

REGULATION OF KATANIN ACTIVITY ON MICROTUBULES

SEPTEMBER 2017

MADISON A. TYLER, B.S., UNIVERSITY OF MASSACHUSETTS AMHERST

M.S., UNIVERSITY OF MASSACHUSETTS AMHERST

Directed by: Jennifer Ross

The cytoskeleton is a dynamic network of microtubules constantly being reorganized to meet the spatiotemporal demands of the cell. Microtubules are organized into subcellular highways to control cell processes such as cell division, cargo transport, and neuronal development and maintenance. Reorganization of this intricate network is tightly regulated by various stabilizing and destabilizing microtubule-associated proteins that decorate the network. Katanin p60 is a microtubule destabilizing enzyme from the ATPases Associated with various Activities (AAA+) family. It can both sever and depolymerize microtubules. In order to sever microtubules, katanin recognizes the tubulin carboxy-terminal tails (CTTs) and hydrolyzes ATP. Using super-resolution microscopy and image analysis, we find that the tubulin CTTs are not required for katanin to depolymerize microtubules. We also characterize the regulation of microtubule severing and depolymerization by katanin in various nucleotide states. A better understanding of how CTTs and nucleotides regulate microtubule severing and depolymerization by katanin will help future research aimed to correct katanin activity when these processes goes awry as in improper chromosome segregation during mitosis or loss of microtubule integrity in neuronal diseases.

TABLE OF CONTENTS

Page

LIST OF FIGURES

Figure Page

CHAPTER 1

INTRODUCTION

1.1 The Cytoskeleton

In order to function properly, the cell must coordinate itself in a spatiotemporal manner. The cell must change shape, move, and be able to reorganize its components. Hundreds of cellular processes occur in a given day, therefore cells must be highly dynamic in order to coordinate these processes and meet their immediate needs for survival. Eukaryotic cells have evolved to become very good at coordinating essential cell processes that depend on the cytoskeleton, a complex network of filaments. One component of the cytoskeleton is microtubule filaments. Microtubules are critical components to important cellular processes including cell division, neuronal maturation, and intracellular transport (Sharp & Ross, 2012). Microtubules are so essential that almost any mutation in microtubules results in death (one results in blindness only) (Tischfield, Cederquist, Gupta, & Engle, 2012).

One example of rapid and seamless reorganization of microtubules is in a healthy cell undergoing cell division. After chromosomes and other cellular organelles are duplicated, the microtubules of the cell organize themselves into bipolar mitotic spindles. In this arrangement, microtubules extend out from the microtubule organizing center and attach to chromosomes at the kinetochore (Tanaka & Desai, 2008). These microtubules are responsible for proper segregation of chromosomes into daughter cells. After cell division, the two daughter cells should contain one copy of each chromosome. The cell even has error correction pathways to biorientation in which sister kinetochores attach to dynamic microtubules from opposite spindle poles (Ye & Maresca, 2015). However, when the microtubule array fails to properly segregate the chromosomes, this

can lead to conditions defined by aneuploidy, where the cell has too many or too few copies of a chromosome. One such condition is Down's Syndrome.

Tight regulation of the microtubule network is essential to avoid the disease states that can arise when microtubules are misregulated. Microtubule-associated proteins (MAPs) are proteins that control the assembly of microtubule filaments. They are responsible for creating new interactions between proteins and breaking interactions with other proteins to ensure the success of the cellular process. There are many types of MAPs, with jobs such as promoting nucleation, promoting and speeding up growth, guarding against catastrophe (switching between growth state and a shrinkage state), promoting catastrophe, speeding or slowing depolymerization, promoting rescue (switching between shrinkage state and the growth state), bundling microtubules, crosslinking microtubules, moving microtubules relative to each other, stiffening microtubules, or spacing microtubules.

For example, tau is a MAP abundant in neurons and promotes microtubule assembly and stabilization while is also spaces and stiffens microtubules (Hawkins, Sept, Mogessie, Straube, & Ross, 2013; Paglini, Peris, Mascotti, Quiroga, & Caceres, 2000; Ross, Santangelo, Makrides, & Fygenson, 2004). Kinesin-5 is a microtubule crosslinking and transporting motor enzyme that encourages polymerization by sliding antiparallel microtubules during spindle assembly and regulates nascent axon branching (Chen & Hancock, 2015; Kapoor, Mayer, Coughlin, & Mitchison, 2000; Nadar, Ketschek, Myers, Gallo, & Baas, 2008). Of the destabilizing proteins, all are enzymes that use ATP. Some are from the kinesin-family. An interesting family of destabilizing proteins, is the microtubule severing enzymes, including katanin, spastin, and fidgetin. Although the mechanism of severing remains poorly understood, these enzymes play crucial roles in major cellular processes including chromosome segregation in mitosis, neurogenesis,

cilia control, and spindle scaling (Hu, Wen, Pomp, Oz, Ben-Omran, Tawfeg, Kodani, Andrew, Henke, Katrin, Mochida, Ganeshwaran H., Yu, Timothy W., Woodworth, Mollie B., Walsh, 2015; Loughlin, Heald, & Nédélec, 2010; Loughlin, Wilbur, McNally, Nédélec, & Heald, 2011; Sharp & Ross, 2012; Zhang, Rogers, Buster, & Sharp, 2007).

1.2 Microtubules

Microtubules are hollow cylinders made of the protein tubulin. They vary in length, but can be as long as 50 µm *in vivo*. The microtubule polymer is made up of alpha and beta subunits. One alpha and one beta subunit come together to form a dimer of 110 kilodaltons. The alpha-beta dimers assemble into protofilaments that bind side-to-side to form a sheet that rolls into a tube with 13-protofilaments around (Fig. 1). The microtubule measures 25 nm in width in the outer diameter, with the hole down the center about 17 nm is diameter. The hollow center gives microtubules a rigid structure that results in a long persistence length, a mechanical property based on the stiffness of the polymer.

Each microtubule has structural asymmetry and has a plus end and a minus end. Tubulin dimers associate with one another such that the alpha subunit comes into contact with a beta subunit of another dimer that is already part of the microtubule lattice. The dimers always bind with the same directionality which causes structural polarity. Thus, there is a microtubule end with a ring of beta tubulin, named the plus end, and a microtubule end with a ring of alpha tubulin, named the minus end (Fig. 1).

Changes in microtubule length are driven by GTP-hydrolysis at the plus end of the microtubule (Mitchison, 1993). Both alpha and beta tubulin have GTP-binding sites, however the alpha tubulin GTP-binding site is called non-exchangeable and the beta tubulin GTP-binding site is called exchangeable. After polymerization, the GTP in the

exchangeable site is hydrolyzed and becomes nonexchangeable (Nogales, 1999; Nogales, Whittaker, Milligan, & Downing, 1999). This makes the body of the microtubule GDP-tubulin that energetically favor depolymerization. Thus, the microtubule will continue to grow as long as the ring of GTP-tubulin remains at the plus-end. This is called the GTP cap. Evidence for the GTP cap comes from experiments with the nonhydrolyzable GTP analogue GMPCPP that show that GTP-tubulin is stable in the cylinder structure (Hyman, Salser, Drechsel, Unwin, & Mitchison, 1992). However, when the GTP cap is lost, the microtubule rapidly depolymerizes or undergoes catastrophe. This constant flux of microtubule growing and shrinking is called dynamic instability and is an important inherent property of microtubules (Mitchison & Kirschner, 1984).

In our experiments, microtubules are stabilized with Taxol. Taxol is a chemotherapeutic drug used in cancer patients and patients with neurological diseases where microtubules are not properly regulated (Arnal & Wade, 1995). Taxol stabilizes microtubules by binding to a site that is different from the GTP-binding site and prevents microtubule catastrophe. We also have not added free tubulin dimers and GTP to these assays, which prevents polymerization. We restrict the inherent ability of the microtubule to grow and shrink because we want to study just the activity of katanin on microtubules.

Each alpha and beta tubulin monomer has a negatively charged carboxy-terminal tail (CTT) which makes the microtubule negatively charged on its surface. Alpha and beta CTTs are extremely important to the microtubule structure. The alpha and beta tails are different and can be post-translationally modified in the cell. This is important because many enzymes are thought to recognize the microtubule through its CTT, including the severing enzymes (Bailey, Sackett, & Ross, 2015; Valenstein & Roll-Mecak, 2016). In fact, our lab has found that katanin preferentially binds to the beta CTT (Bailey et al., 2015). We can study the effects of the carboxy-terminal tail by cleaving it

with a protease called subtilisin (Bhattacharyya, Sackett, & Wolff, 1985). Therefore, we can polymerize microtubules in a test tube and cleave off the CTT, leaving just the hollow cylinder structure.

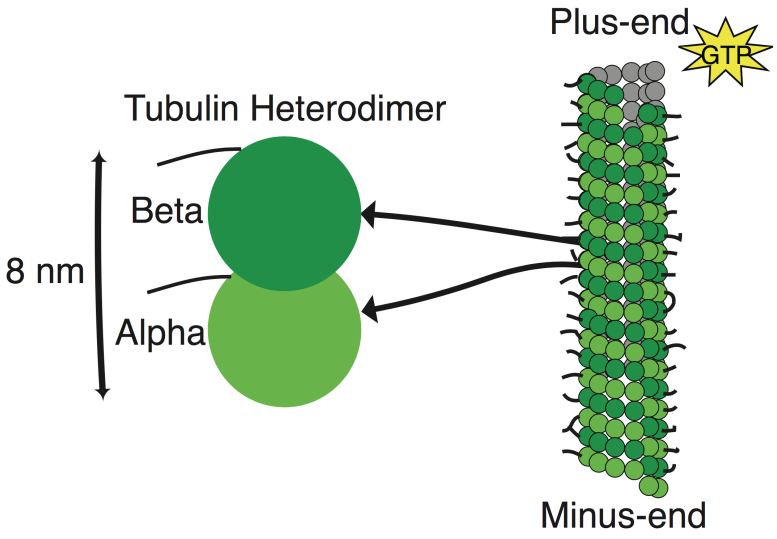

Figure 1. Microtubule Structure.
Microtubules are dynamic filaments composed of dimers of alpha and beta subunits. Tubulin dimers associate with one another such that the alpha subunit comes into contact with a beta subunit of another dimer that is already part of the microtubule lattice. This gives the microtubule polarity with a beta tubulin ring at the plus end and an alpha tubulin ring at the minus end. The GTP-bound beta tubulin ring at the plus end is called the GTP cap. The presence or absence of this cap drives dynamic instability, the inherent property of microtubules to grow and shrink.

1.3 Microtubule Severing Enzymes

In healthy cells, microtubule dynamics are coordinated in space and time by stabilizing and destabilizing MAPs. The microtubule severing enzymes are important destabilizing MAPs. There are three severing enzymes named katanin, spastin, and fidgetin. They are ATPases Associated with diverse cellular Activities (AAA+ family proteins) and are involved in many cellular processes because of their roles in regulation of microtubule networks (Roll-Mecak & McNally, 2010; Sharp & Ross, 2012). When the severing enzymes are mutated or improperly regulate microtubules, disease states can occur. One disease state that can occur is hereditary spastic paraplegia, which is characterized by progressive weakness and stiffness of the legs. The most commonly mutated gene to cause hereditary spastic paraplegia is the spastin gene (Hazan et al., 1999). Studying these enzymes is certainly important and research may lead to new insights as to how to treat these diseases. Future work may allow us to use severing enzymes as a tool to target specific microtubules for reorganization to help people with these disorders.

Our lab is particularly interested in the severing enzyme katanin. Katanin has been implicated in many important cellular processes including meiotic spindle shape and size, mitotic progression, cytokinesis, cilia biogenesis, and neuronal processes (Ahmad, Yu, Mcnally, & Baas, 1999; Loughlin et al., 2011; Matsuo et al., 2013; Rogers, Rogers, & Sharp, 2005; Sharma et al., 2007). Ultimately, our lab aims to elucidate the mechanism of katanin activity on microtubules. There are two types of activity katanin can have on microtubules: severing and depolymerization (Fig. 2). Katanin severs microtubules by localizing to the CTT of tubulin and removing a tubulin dimer somewhere in the middle of the microtubule to create two shorter microtubules. In depolymerization, katanin loosens tubulin dimers from either end of the microtubule and

the same microtubule gets shorter. Less is known about mechanism of katanin depolymerization on microtubules.

The amino-termini of the three enzymes are different. Katanin contains a microtubule interacting and trafficking (MIT) domain in its amino-terminus, which enables it to dock onto the microtubule (Fig. 3). In human katanin the MIT has been mapped to amino acids 55-180 (Eckert, Le, Link, Friedmann, & Woehlke, 2012; Mcnally & Thomas, 1998). At the far end of the amino-terminus is the katanin p80 interacting region. Katanin p80 is the regulatory protein of katanin p60 (McNally, Bazirgan, & McNally, 2000). It regulates katanin p60 by modulating severing activity and directing p60 severing activity in the cell. Our assays contain only katanin p60.

The severing enzymes have sequence and structural similarities that enable activity on microtubules. Their similar carboxy-terminal AAA domains are responsible for the catalytic activity. The AAA domain hydrolyzes ATP and uses the chemical energy of ATP to translate into mechanical energy of severing. The AAA domain contains the Walker A motif, which is responsible for ATP binding and the Walker B motif, responsible for ATP hydrolysis (Frickey & Lupas, 2004) (Fig. 3). In our assays, a Walker B mutant katanin can bind to but not hydrolyze ATP. We use the Walker B mutant katanin to explore the role of ATP in katanin's ability to bind to microtubules. The AAA domain of katanin also contains 2 identified pore loops (Eckert et al., 2012; Johjima et al., 2015; Mcnally & Thomas, 1998; Zehr et al., 2017). An aromatic amino acid residue is highly conserved in one of the pore loops of most AAA+ proteins and is amino acid 282, a tyrosine, in human katanin (Johjima et al., 2015). Interestingly, spastin has 3 pore loops, compared to katanin's 2 known pore loops (Roll-Mecak & Vale, 2008; White, Evans, Lary, Cole, & Lauring, 2007). The conserved pore loops of AAA+ proteins are crucial to the protein carrying out its function in the cell.

Each katanin monomer contains these MIT and AAA domains (Fig. 3). In the cell, katanin monomers oligomerize into a hexamer on a microtubule in the presence of ATP (Hartman & Vale, 1999). However, whether hexamerization occurs before or after microtubule binding remains unknown. Once hexamerization happens, a small pore is formed in the middle of the enzyme where the positively charged pore loops are located. The pore of the assembled hexamer is thought to interact with the CTT and that starts the reaction of microtubule severing by some unknown mechanism. Two mechanisms have been proposed, however, and they are primarily based on a model that we on spastin severing (Roll-Mecak & Vale, 2008; White et al., 2007). One is that the tubulin is unfolded and translocated through the center pore, like in other AAA+ enzymes like ClpX (Iosefson, Olivares, Baker, & Sauer, 2015). The other suggested mechanism is that tubulin-tubulin interactions are destabilized when the positively charged pore loops tug on the CTT, releasing the tubulin dimer from the lattice.

Previously, lack of 3D structures of katanin made elucidating the severing activity difficult. There has been a crystal structure of spastin with a 3D envelope structure from small-angle x-ray (Roll-Mecak & Vale, 2008). This spastin structure was used as the structural basis for katanin, as well. A very recent paper has recently shined new light on the structure and possible mechanism of action of katanin (Zehr et al., 2017). They found that via ATP hydrolysis, katanin can cycle between two conformations: open spiral and closed ring. Open spiral conformation is when there is a gap between katanin monomer 1 and 6. In this conformation, the hexamer is open and the pore loops are not all engaged with the CTT of tubulin. Closed ring conformation occurs when subunit 1 and 6 make contact and the katanin hexamer is closed (Fig. 4). In this conformation, the pore loops of all monomers are engaged with and can tug on the CTT. This new article suggests that the cycling of the hexamer between open and closed conformations

creates the power stroke for microtubule severing (Zehr et al., 2017). More research should be conducted to better understand this proposed mechanism of katanin severing.

Katanin was the first microtubule severing enzyme discovered (Vale, 1991) yet its mechanism of severing remains elusive. Our lab has had previous success purifying and studying katanin. We determined 1) katanin targets microtubule defects (Diaz-Valencia et al., 2011), 2) free tubulin inhibits katanin activity (Bailey et al., 2015), 3) katanin prefers beta tubulin tails to alpha tubulin tails (Bailey et al., 2015), 4) ATP concentration affects katanin activity (unpublished data). This is an exciting time to be studying katanin, as a partial structure of katanin p60 in *C. elegans* has just been solved (Zehr et al., 2017). Yet, even with the structure and research that has been conducted thus far, many questions remain. We are interested in further elucidating the mechanism of katanin activity on microtubules. Using *in vitro* microtubule severing assays and TIRF microscopy, we aim to answer some of these important questions to better understand how microtubules are coordinated in space and time.

A. Katanin Severing a Microtubule

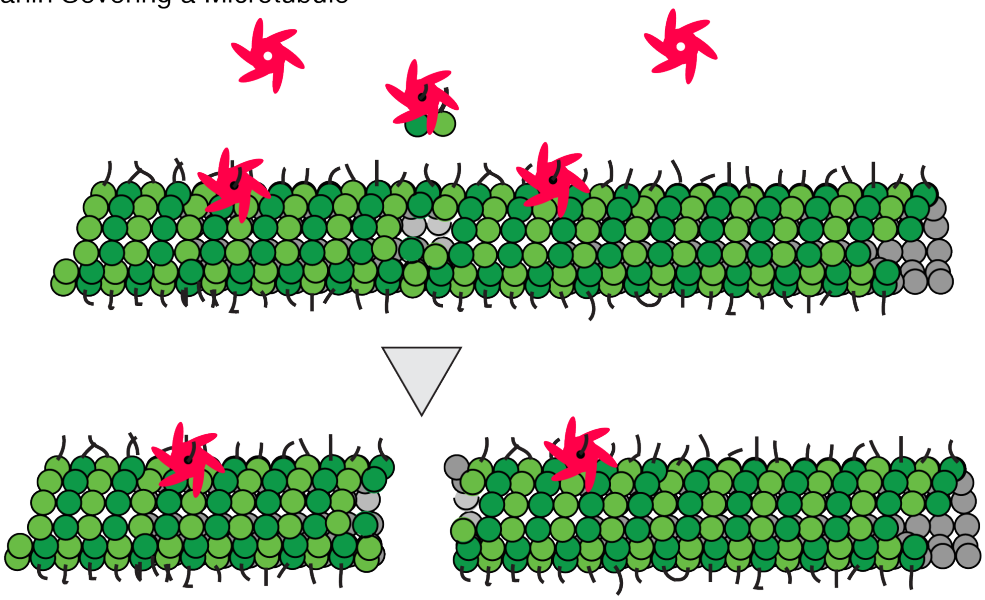

B. Katanin Depolymerizing a Microtubule

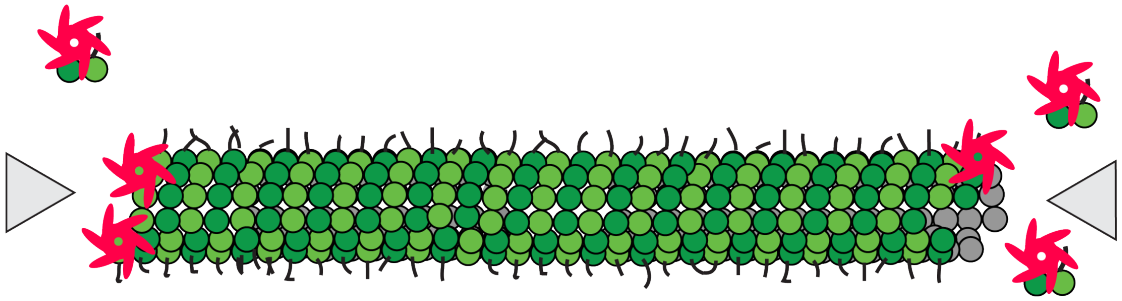

Figure 2. Katanin Severing and Depolymerization Activity on Microtubules.
Katanin can either A) sever or B) depolymerize microtubules. In severing, katanin hexamerizes on a CTT in the middle of the microtubule to remove a tubulin dimer. The removal of a dimer induces a break in the microtubule lattice, causing two shorter microtubules to form. In depolymerization, katanin loosens tubulin dimers from either end of the microtubule. These mechanisms are thought to be distinct and regulated differently.

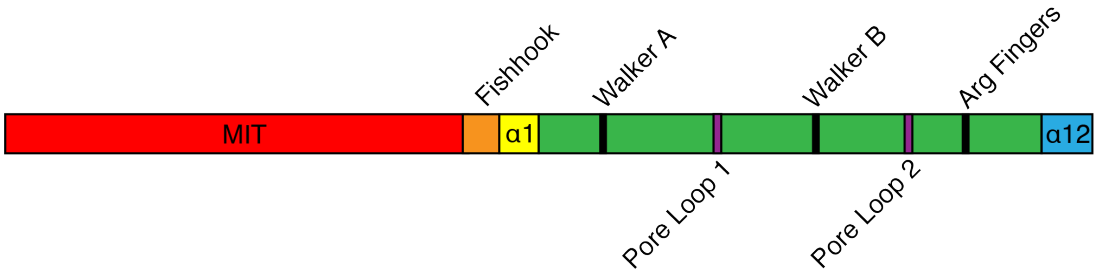

Figure 3. Domain Diagram of Katanin p60.
The microtubule interacting and trafficking (MIT) domain is located at the carboxy-terminus (red). A fishhook region (orange) located on the microtubule-interacting side near the MIT domain is probably one of the first structural elements to interact with the microtubule. The alpha 1 (yellow) and alpha 12 (blue) helices act as linkers to the fishhook region structurally linking the microtubule-binding face of katanin with the outward face of katanin. The AAA domain contains also the Walker A and B regions (black) for ATP binding and hydrolysis, respectively. Katanin contains arginine fingers (black) that contact ATP phosphates. The pore loops are located in the AAA domain as well (purple).

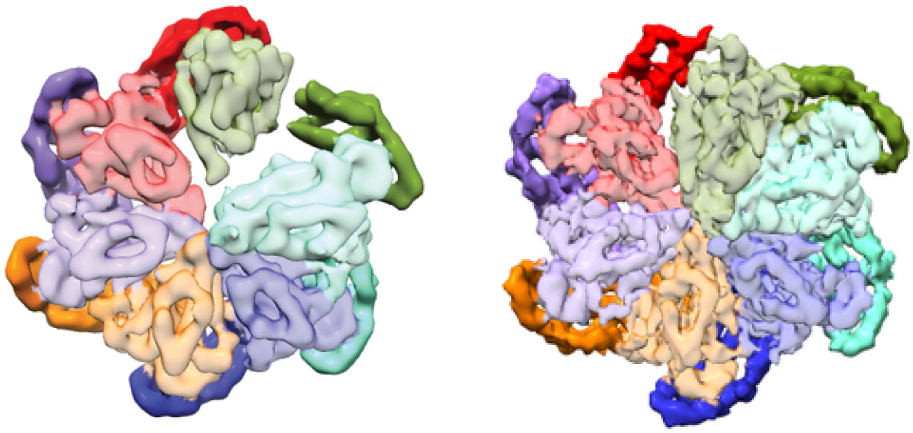

Figure 4. 3D Models for Katanin Hexamer in the Ring Conformation.
Katanin p60 in closed ring conformation. In this conformation, each of the six subunits interface and the pore loops in the center of the protein are engaged with the CTT of tubulin (PDB, Zehr et al., 2017).

1.4 Biophysics of Microtubules

Biophysics, or biological physics, is an inherently interdisciplinary field where the techniques and theories of physics are used to study biological processes. Our lab is a biophysics lab that uses high-resolution microscopy to study microtubules and their associated proteins and enzymes. We use methods of physics to collect, analyze, and present the data. This is a useful way to study microtubules and other aspects of biology for several reasons. 1) Biology is traditionally a qualitative field, yet using physics to study these processes allows us to quantify inherently qualitative biological processes. This is important because it allows us to share unsubjective, verifiable results. 2) Biology and physics are not two mutually exclusive disciplines. The laws of physics apply in biology and therefore it is important to study biological processes with physics. 3) We can answer more interesting questions with greater depth with interdisciplinary work. Our lab is highly collaborative and interdisciplinary and as such, biologists and physics interact daily to answer important questions about the regulation of microtubules.

In this thesis, I aim to describe how I employed biophysical techniques to better understand katanin's role in microtubule regulation. I use total internal fluorescence microscopy with single molecule sensitivity to study katanin's interactions on single microtubules. Specifically, this thesis elucidates katanin's mechanism of binding to the microtubule and to further distinguish its severing activity from depolymerization activity on microtubules. Presently, this work will provide new insight to important questions about the mechanism of severing enzymes on microtubules and how microtubules are organized by this mysterious protein. In the future, this work will help us answer complex questions about entire microtubule networks and how other proteins interact with katanin to regulate microtubules in cells.

CHAPTER 2

ATP CONCENTRATION REGULATES KATANIN ACTIVITY

2.1 Introduction

ATP is an important energy source for many proteins, including microtubule severing enzymes. Severing enzymes convert the chemical energy from ATP to mechanical energy to sever microtubules (Eckert et al., 2012; Hartman & Vale, 1999; Roll-Mecak & Vale, 2008). Although it is known that katanin requires ATP to sever microtubules, the amount of ATP required has not been explored. Our assays normally contain 2 mM ATP, which is often considered within the range of physiological concentration of ATP. However, the cell is highly transient with hundreds of thousands of molecules shifting and interacting at once. Local concentration gradients are in constant flux (Ross, 2016).

Work in our lab by a former graduate student performed an ATP scan to test the activity of a *X. laevis* katanin. She performed experiments with 28 µM, 100 µM, 500 µM, 1 mM, 2 mM, 5 mM, 10 mM, and 20 mM ATP. She found that the loss of polymer increased as the concentration of ATP is increased, up to a certain point (Fig. 5). Interestingly, the loss of polymer was due to different mechanisms at low and high ATP concentrations: microtubule depolymerization at low concentrations of ATP and microtubule severing at medium concentrations of ATP (Fig. 5A). Severing is expected at 1 mM and 2 mM because this is the concentration of ATP typical in our microtubule severing assays and prior work (Bailey et al., 2015; Eckert et al., 2012; Loughlin et al., 2011; Valenstein & Roll-Mecak, 2016). As the concentration of ATP was increased beyond 2 mM ATP, however, activity on microtubules ceased (Fig. 5B). This data is interesting because it suggests ATP may play a role in regulating katanin activity.

This prior work was not yet published because we used an unlabeled version of katanin, which did not allow us to directly monitor the binding of katanin to microtubules. It is possible that the katanin was not severing because it was not binding to microtubules at high ATP concentration. To better understand the role of ATP concentration in regulating katanin activity on microtubules, we performed an ATP scan using a GFP-labeled human katanin in a microtubule severing assay. We performed experiments with 28 μM, 100 μM, 500 μM, 1 mM, 2 mM, 5 mM, 10 mM, and 20 mM ATP, as before. Using this fluorescently-labeled human katanin, we were able to study the characteristics of katanin binding to microtubules.

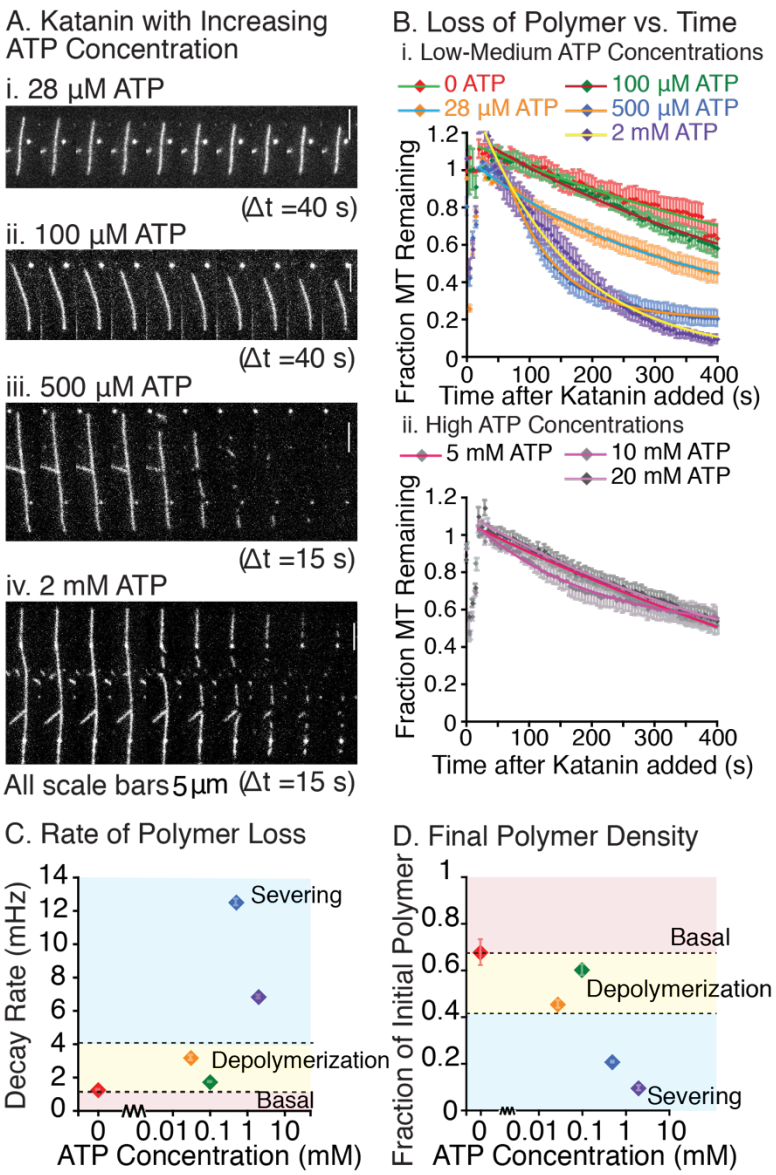

Figure 5. Katanin Activity on Microtubules is Dependent on Concentration of ATP. Previous work by Megan Bailey from our lab found that katanin activity on microtubules is dependent on concentration of ATP. A) Time series of katanin activity on microtubules at low-medium concentrations of ATP. B) Quantification of total loss of polymer over time shows that the fraction of microtubules remaining decreases as the concentration of ATP increases from low to medium levels. However, at higher concentrations of ATP, including 5 mM, 10 mM, and 20 mM ATP, katanin activity is reduced. C) Quantification of rate of polymer loss and D) final polymer density show that there are three phases of katanin activity on microtubules. This includes the basal phase where little to no polymer is lost, the depolymerization phase where polymer is lost only from the ends of microtubules, and the severing phase where katanin severs microtubules.

2.2 Methods

2.2.1 Protein Purification

The pMAL-c2x human p60 construct containing an ampicillin resistance sequence was created in our lab. It contains a maltose binding protein for purification and a sfGFP tag for visualization in TIRF microscopy. We used an IPTG inducible expression system to express and purify katanin. The plasmid was transformed into BL21 competent *E.coli* cells (New England BioLabs) and plated with carbenicillin, an ampicillin-like molecule with improved stability in growth media. A starter culture containing a single colony and a 1:1000 dilution of carbenicillin to Lysogeny broth (LB) was incubated at 37°C overnight and added to a 400 ml culture the next day. This culture was grown at 37°C until it reached an OD of 0.8 and then it was induced with 1 mM IPTG. The culture was allowed to continue to grow at 16°C for 16 hours. Cells were pelleted then lysed in resuspension buffer (20 mM Hepes pH 7.7, 250 mM NaCl, 0.5 mM BME, 10% glycerol, 0.25 mM ATP) via sonication. The lysate was incubated at 4°C with amylose resin (New England BioLabs) for 1.5 hours to encourage maltose binding protein to bind to amylose. Next, the mixture was added to the column and allowed to enter the column completely. Once excess lysate had passed through the column, the column was washed with 20 ml of resuspension buffer (20 mM Hepes pH 7.7, 250 mM NaCl, 0.5 mM BME, 10% glycerol, 0.25 mM ATP). Then the protein was eluted in elution buffer which contains maltose, for which maltose-binding protein has a higher affinity (20 mM Hepes pH 7.7, 250 mM NaCl, 0.5 mM BME, 10% glycerol, 0.25 mM ATP, 10 mM Maltose). The approximate concentration of katanin was measured by a Bradford assay. Later, the exact concentration was found using SDS-PAGE gel analysis.

2.2.2 Katanin Storage

Directly after purification, we tested katanin to find the working concentration. We then added glycerol to 50%, aliquotted, drop froze in liquid nitrogen, and stored at -80°C. It was previously believed that katanin could not be stored because of total loss of activity. However, we found that purified katanin in 50% glycerol could be saved up to 1 month after the date of purification with minimal activity loss if used within this time period.

2.2.3 Taxol-stabilized Microtubule Polymerization

Taxol-stabilized microtubules were made by combining a 1:10-1:20 ratio of labeled rhodamine tubulin (Cytoskeleton) or homemade Dylight 649 (Thermo Scientific) tubulin with unlabeled tubulin (Cytoskeleton). Both the unlabeled and labeled tubulin were resuspended in PEM-100 (100 mM K-Pipes, pH 6.8, 2 mM MgSO4, 2 mM EGTA) to a concentration of 5 mg/ml (45.5 µM). Both were incubated on ice for 10 minutes. The labeled and unlabeled tubulin were combined to the appropriate ration and centrifuged at 366,000 xg, 4°C for 10 minutes. To polymerize the microtubules, 1 mM GTP was added to the tubulin and it was incubated at 37°C for 20 minutes. To further stabilize the microtubules, 50 µM Taxol was added and incubated for another 20 minutes at 37°C. The microtubules were centrifuged at 16,200 xg, 25°C for 10 minutes. The pellet was resuspended in PEM-100 and 50 µM Taxol. The microtubules were sheared with a Hamilton syringe and incubated at 37°C overnight for a maximum of three nights.

2.2.4 In vitro assays

A 10 µl flow chamber was made with double stick tape, a coverglass (Fisherbrand) and a coverslip (Fisherbrand) that was treated with Ultra Violent light and Oxygen plasma (UVO) and silane (Dixit & Ross, 2010). The coverslips were UVOed for

20 minutes. Coverslips were then coated with 2% dimethyldichlorosilane (GE Healthcare) to create a hydrophobic surface to enable specific binding of hydrophobic proteins and polymers. The surface of the chambers were made to specifically bind microtubules by first incubating 2% (w/v) MAB1864 tubulin antibody in Katanin Activity Buffer (20 mM Hepes pH 7.7, 10% glycerol, 2 mM MgCl2) for 5 minutes. Then 5% (w/v) Pluronic F-127 in Katanin Activity Buffer (20 mM Hepes pH 7.7, 10% glycerol, 2 mM MgCl2) was added to block the surface. Next, a 1:50-1:100 dilution of Taxol-stabilized Rhodamine or Dylight 647 microtubules in PEM-100 were incubated in the chamber for 5 minutes. To remove excess unbound microtubules, Katanin Severing Buffer (Katanin Activity Buffer with 2 mM ATP, 0.025 mg/mL BSA, 0.05% F-127, 10 mM DTT, 15 mg/mL glucose, 0.15 mg/mL catalase, 0.05 mg/mL glucose oxidase) was washed through the chamber. After 30 seconds of imaging, Katanin Severing Buffer with p60 (usually 100-400 nM GFP-p60) was added.

Three videos of 10 different conditions for a total of 30 same-day videos were collected. All concentrations were kept the same except for ATP concentration. In these assays, a constant concentration of 250 nM katanin was maintained and only the concentration of ATP-Mg^{2+} (Sigma) was adjusted. The concentrations of ATP-Mg^{2+} were 28 μM, 100 μM 500 μM, 1 mM, 2 mM, 5 mM, 10 mM, and 20 mM. There was also a 2 mM ATP-γ-S (Jena Bioscience) control and a control without katanin. Montages of the conditions are shown below (Fig. 6,9,11). An image was taken before and after each video in the EPI fluorescence to compare the state of the microtubules since intense laser illumination can photodamage microtubules.

2.2.5 Microscopy

Data was collected with a home-built, single molecule total internal reflection fluorescence laser system. The microscope is a Nikon Ti-E with automated fluorescence turret and z-scanner with Perfect Focus. A 60x objective (NA 1.49) is used for total internal reflection fluorescence (TIRF) microscopy. The microscope has an Intenselite XeHg light source and light guide for illumination in the epi-fluorescence path. The microscope has dichroic cubes for TIRF and epi-fluorescence emission in green, red, and far-red wavelengths. The blue (488 nm, 50 mW) TIRF laser was used to excite the GFP-labeled p60. The microscope system is run by a Windows PC computer using Nikon Elements software. This software allows the automation of fluorescence, exposure, and shutters to the sample. The software also runs the cameras, of which the lab has two. This system has an Andor EM-CCD for single molecule imaging. There was a 2.5x magnifier in front of the camera resulting in a 108 nm effective pixel size.

All images were obtained using identical camera, microscope, and lens hardware. All same day imaging criteria such as gain, ND filters, and exposure time was kept the same and efforts were made to minimize differences across data sets. Efforts were made to ensure that the images were not saturated and that minimal bleaching of the fluorescence occurred before image acquisition. Same day controls were performed to address photobleaching. Digital gray values of image pixels representing arbitrary fluorescence units (AFUs) were obtained using Nikon Elements software. Fluorescence intensity was quantified for fluorescently labeled microtubules and GFP-katanin to quantify severing and binding, respectively.

2.2.6 Katanin Binding Analysis

Katanin binding analysis was performed in ImageJ. Movies were taken without delay between frames for 10 minutes in the 488 nm TIRF channel to assess katanin activity on microtubules. An image was taken of the microtubules before and after the movie to ensure photodamage did not occur while imaging. In conditions where there were a low levels or no binding to the microtubule, before images showed exactly where to measure in the TIRF channel. We used the line tool to draw a segmented line over the entire length of the microtubule. The Multi Measure plugin was used to measure multiple microtubules (or ROIs). The mean intensity of each microtubule was measured over time during the time series. A line of the same length was moved off of the microtubule to measure the background intensity near the microtubule to assess background noise. The intensity on the microtubule was divided by the intensity in the background to get the signal to noise ratio for each frame. That value was subtracted by 1. The data from many microtubules in the same experimental parameters were averaged together. The maximal GFP fluorescence was determined from the averaged data. Data were fit over time, and the association rate, oligomerization rate, and severing rate were determined by fitting the data.

2.2.7 SDS-PAGE Gel Analysis

Purified katanin was quantified by SDS-PAGE gel and analysis using ImageJ. The amount of protein in each well totaled less than 1 µg, because this is the limit beyond which Coomassie staining cannot resolve. The intensity of the bands for the BSA standards were plotted and fit to a line to determine the linear regime of Coomassie staining. Only protein dilutions within this linear regime were used to calculate the concentration of katanin. Several dilutions were in the linear regime of the BSA

standards. Using a molecular weight of 126 kD and the known volume and dilution of the sample loaded into each gel well, we calculated a yield of 5.3 μM katanin. This is similar to the 6.3 μM of protein calculated via the Bradford assay. Minimal impurities were seen on the Coomassie gel.

2.3 Results

2.3.1 Katanin Binds to and Severs Taxol-stabilized Microtubules in the Presence of ATP

It is well-known that katanin requires ATP to sever microtubules. Yet, it is necessary that we check the activity of katanin on Taxol-stabilized microtubules. Previous studies have shown that katanin can sever Taxol-stabilized microtubules *in vitro* (Bailey et al., 2015; Diaz-Valencia et al., 2011; Eckert et al., 2012; Loughlin et al., 2011; Mcnally & Thomas, 1998; McNally et al., 2014; McNally et al., 2000; Whitehead, Heald, & Wilbur, 2013; Zhang et al., 2011). In our assays, we always perform a control to test the activity of katanin, as each preparation of protein shows slightly different activity. Some preps are highly active while others are only moderately active. This also demonstrates that our protein is indeed functioning as expected and there are no functionally silent mutations in katanin. In our experience, katanin is prone to collecting mutations that disrupt its severing ability.

The concentration range of ATP for which severing occurred was 500 μM to 2 mM (Fig. 6B,C,D). We conclude also that this is an active batch of protein, as total severing of microtubules occurs in around 130 seconds in the presence of 2mM ATP (Fig. 6D). This is important for the assay because we want to measure katanin binding to microtubules before photobleaching occurs. In control assays without any katanin present, no microtubule binding occurs and no microtubule severing occurs (Fig. 6A). However, we see the effect of some photobleaching on microtubules in our after picture of microtubules after illuminating them with 488 nm laser for 10 minutes (Fig. 8A,B). We have controlled for this photobleaching to make sure that it is not a product of katanin activity or some other enzyme by taking a picture of the same chamber in a different location (Fig. 8C). Here we see no microtubule damage. Therefore, we can conclude

that the loss of signal to microtubules in this control is due to the laser and not enzymatic activity.

We quantified the amount of katanin bound to microtubules over time (Fig. 7A). The data can be categorized into three phases: binding phase, oligomerization or constant phase, and decay phase. The data before the decay phase was masked and the decay phase data was fit to a single exponential in the form:

$$\mathbf{I(t) = Aexp(-t/\tau)\ (Eq\ 1)}$$

where I is intensity as a function of time, t, and τ is the characteristic decay constant. The characteristic decay constant provides information about katanin activity on microtubules and is also influenced by photobleaching. We determined the characteristic decay constant for 2 mM ATP to be 46 ± 0.1 s. The characteristic decay constant in the presence of 1 mM ATP was similar at 44 ± 0.4 s. However, the characteristic decay constant was only 29 ± 0.3 s in the presence of 500 µM ATP. This suggests katanin activity on Taxol-stabilized microtubules is greatest in the presence of 500 µM ATP. This may be due to an increase in severing events which frees more microtubule ends to be depolymerized.

We then extract the relative maximum GFP (Fig 7B). We measured the relative maximum GFP over microtubules when no katanin is present and determined the value to be 0.04 ± 0.01. This confirms that there is nothing that is GFP-emitting that is interfering with our assays and that nothing is spontaneously binding to the microtubules. The relative maximum katanin bound in the presence of 2 mM ATP is 2.8 ± 0.1. The relative maximum katanin bound was higher for the lower ATP concentrations of 500 µM and 1 mM ATP, both 3.2 ± 0.1. This data suggests katanin binds to microtubules more readily in a range between 500 µM and 1 mM ATP.

We also quantified the time spent in the constant phase, which is the time spent at relative maximum GFP intensity. This constant phase may be the time the enzyme needs to oligomerize and fully bind to the microtubule, and only after this can katanin begin activity on microtubules. The time in this constant phase was only 8 seconds in the presence of 500 μM ATP. At 1 mM ATP it is 17 seconds in the constant phase and at 2 mM ATP katanin is bound in the constant phase for 33 seconds, again demonstrating katanin is most active at 500 μM ATP because the constant phase is shortest. This suggests katanin may oligomerize fastest at this concentration of ATP.

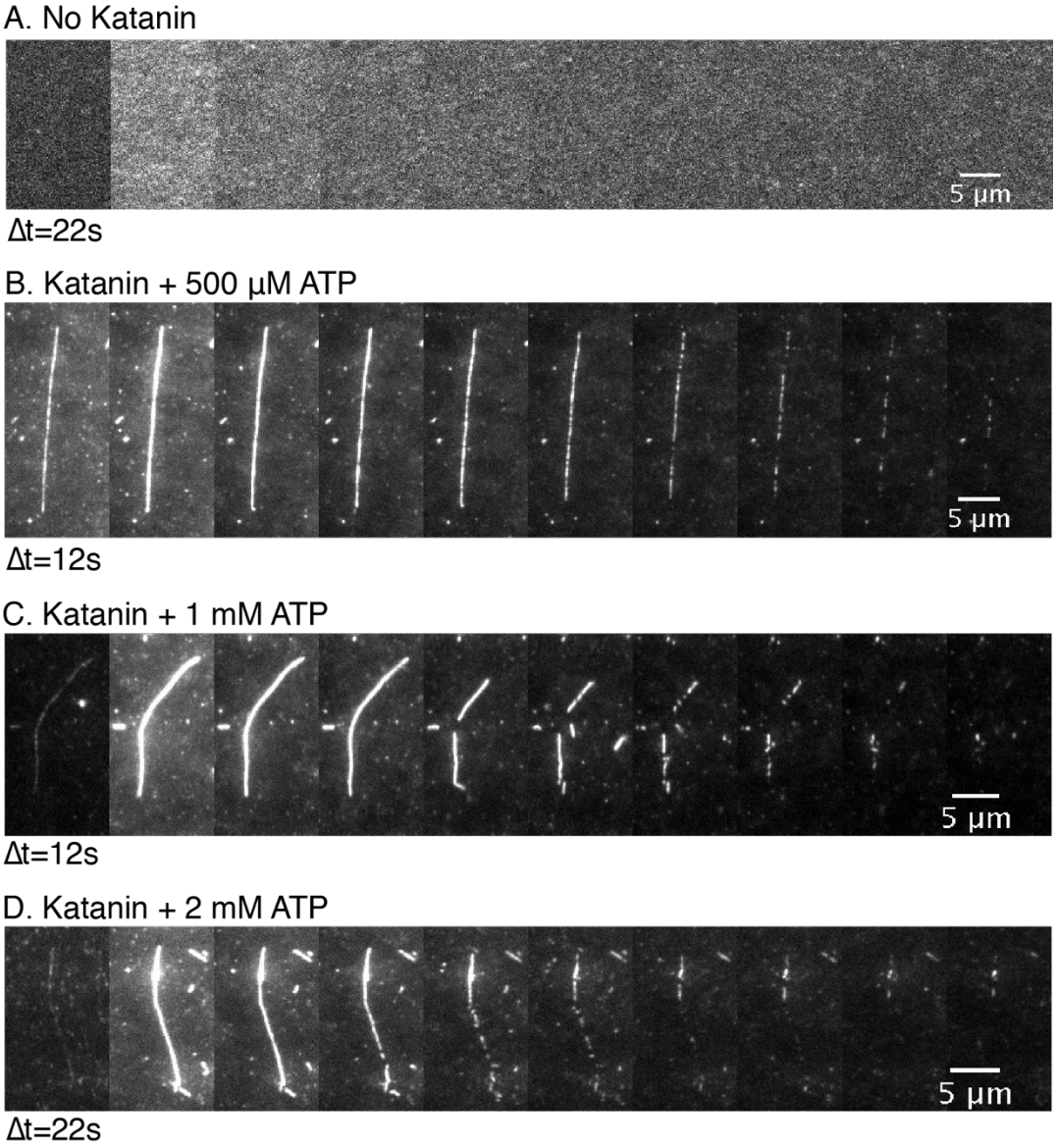

Figure 6. Representative Time Series of Katanin Binding to and Severing Taxol-stabilized Microtubules.

Time series representative of Taxol-stabilized microtubules in a severing assay A) with no katanin and in the presence of katanin and B) 500 µM ATP, C) 1 mM ATP, or D) 2 mM ATP. In the range of 500 µM to 2 mM ATP, katanin binds to and severs microtubules. The time between images is as stated below each time series and all scale bars are 5 µm.

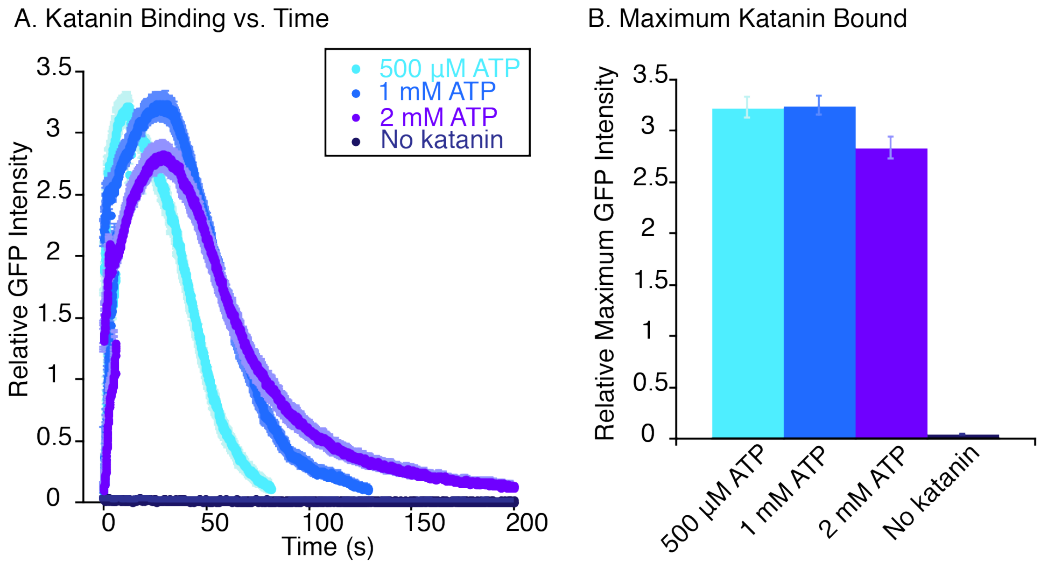

Figure 7. Quantification of Katanin Binding to Taxol-stabilized Microtubules with Moderate Concentrations of ATP.
A) Total katanin bound to microtubules over time for each of the conditions. The first thirty seconds of each video was used as a control to make sure that nothing was binding to the microtubules before GFP-katanin was flown in. Katanin with: 500 µM ATP is light blue (N=43 in 3 different chambers); 1 mM ATP is dark blue (N=103 in 3 different chambers); 2 mM ATP is purple (N=102 in 3 different chambers); and no katanin control is dark purple (N=77 in 3 different chambers). Only in chambers where katanin was present were microtubules completely destroyed throughout the chamber. The error bars are lighter versions of their marker colors and represent the SE. B) Relative maximum GFP intensity from A). Error bars represent ± SE of same microtubules measured in A).

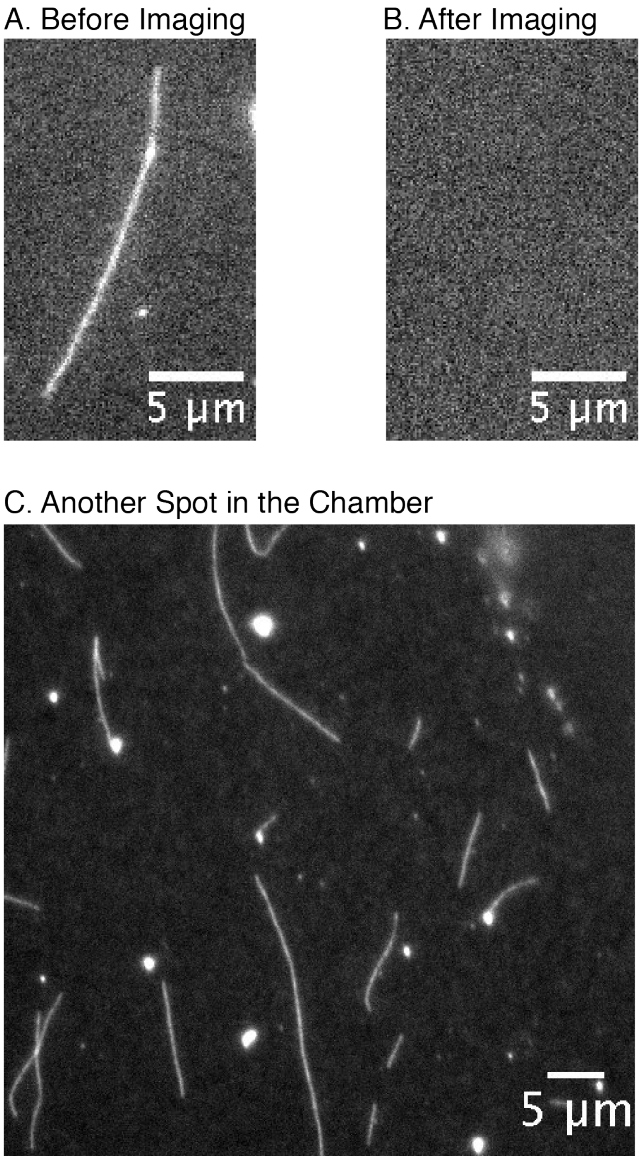

Figure 8. Representative Images of Photobleaching on Taxol-stabilized Microtubules. Images of Taxol-stabilized microtubules without katanin A) before imaging, B) after imaging in the same spot, or C) after imaging in a different location in the same chamber. Microtubules are subject to photobleaching by the 488 nm laser. An image in a different region of the same chamber serves as an important control. All scale bars are 5 µm.

2.3.2 Katanin Depolymerizes Microtubules at Low Concentrations of ATP

We show that katanin binds to microtubules at low concentrations of ATP, including 28 μM and 100 μM ATP (Fig. 9). Qualitatively, the type of katanin activity on Taxol-stabilized microtubules appears similar to that which our lab previously measured (Fig. 5). At 28 μM ATP, katanin is only able to depolymerize microtubules, which is what our lab previously found (Fig. 9A). At 100 μM ATP, the primary activity is depolymerization, however there are some severing events (Fig. 9B). To make sure that katanin activity was the reason for microtubule polymer loss and not the laser, we looked around at different locations in the same chamber and saw no microtubules remaining.

We quantified the amount of katanin bound to microtubules over time (Fig. 10A) and fit the decay phase data to a single exponential decay (Eq. 1) to extract characteristic decay times. We determined the characteristic decay time for katanin on Taxol-stabilized microtubules in the presence of 28 μM ATP and 100 μM ATP to be 121 ± 0.4 s and 111 ± 0.2 s, respectively. The characteristic decay times for katanin on Taxol-stabilized microtubules in the presence of low concentrations of ATP are nearly three times longer than those for moderate concentrations of ATP. Katanin remains bound to microtubules for longer under low concentrations of ATP perhaps because depolymerization activity is slower than when katanin has the ability to sever microtubules. Severing events make new ends for katanin to depolymerize, potentially increasing activity.

We also extracted the relative maximum intensity of GFP-labeled katanin on microtubules (Fig. 10B). Relative maximum intensity for bound katanin was 3.5 ± 0.2 and 3.5 ± 0.1 in the presence of 28 μM ATP and 100 μM ATP, respectively. These values are comparable to values for 500 μM ATP and 1 mM ATP and higher than the 2 mM ATP control, in which case relative maximum GFP intensity is only 2.8 ± 0.1 (Fig. 10B).

This data provides new insight on katanin's depolymerization activity as a function of ATP concentration. It will also help elucidates katanin's mechanism of depolymerization, as it is distinct from severing activity.

2.3.3 Katanin Depolymerizes Microtubules in the Presence of ATP-γ-S

We used ATP-γ-S to study the effect of a non-hydrolyzable ATP-analogue on katanin activity on Taxol-stabilized microtubules. ATP-γ-S has a sulfur instead of oxygen on the gamma phosphate making ATP-hydrolysis difficult for enzymes, including katanin. Prior work has shown that ATP-γ-S inhibits katanin hydrolysis and binding (Eckert et al., 2012). We show that katanin can depolymerizes, but not sever, microtubules in the presence of ATP-γ-S (Fig. 9C). In this sense, the activity of katanin in the presence of 2 mM ATP-γ-S is similar to the activity of katanin in the presence of 28 μM ATP. To get a better sense of katanin activity, we also quantified binding over time (Fig. 10A) and fit the data to a single exponential decay (Eq. 1) to extract a characteristic decay time. We show that in the presence of ATP-γ-S, the characteristic decay time for katanin on Taxol-stabilized microtubules is 181 ± 0.4 s, which is slightly longer than those of the 28 μM and 100 μM ATP conditions. This suggests katanin remains bound to microtubules longer in the presence of ATP-γ-S. The relative maximum GFP-labeled katanin bound to microtubules in the presence of ATP-γ-S is 3.1 ± 0.2 (Fig. 10B). This value is comparable to the values for relative maximum GFP intensity for katanin on microtubules in the presence of low concentrations of ATP. These results suggest ATP-γ-S is a good inhibitor of katanin severing activity but not of depolymerization activity. Because ATP-γ-S inhibits ATP-hydrolysis, perhaps only binding in the ATP-site is required for depolymerization activity.

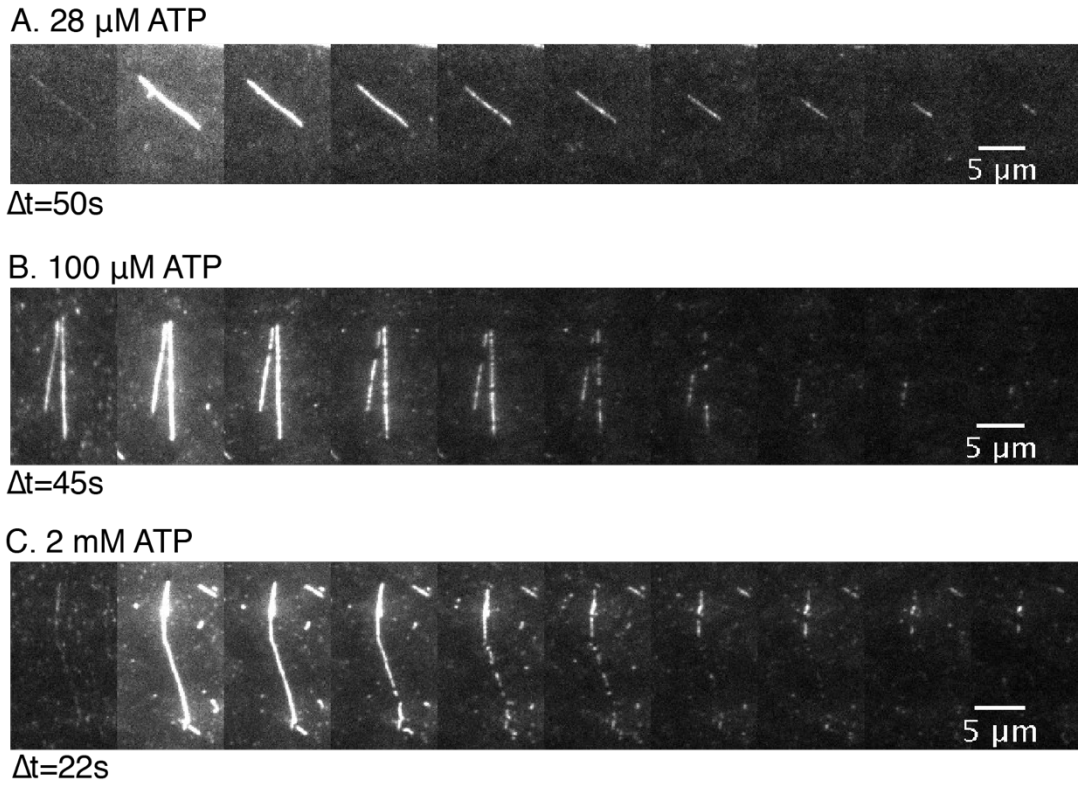

Figure 9. Representative Time Series of Katanin Binding to and Depolymerizing Taxol-stabilized Microtubules.

Time series representative of katanin on Taxol-stabilized microtubules in a severing assay with A) 28 μM ATP B) 100 μM ATP, or C) 2 mM ATP-γ-S. Low concentrations of ATP, from 28 to 100 μM, katanin activity is restricted primarily to depolymerization of microtubules. Some severing occurs at 100 μM ATP. The non-hydrolyzable ATP analogue ATP-γ-S prevents katanin severing but not depolymerization. The time between images is as stated below each time series and all scale bars are 5 μm.

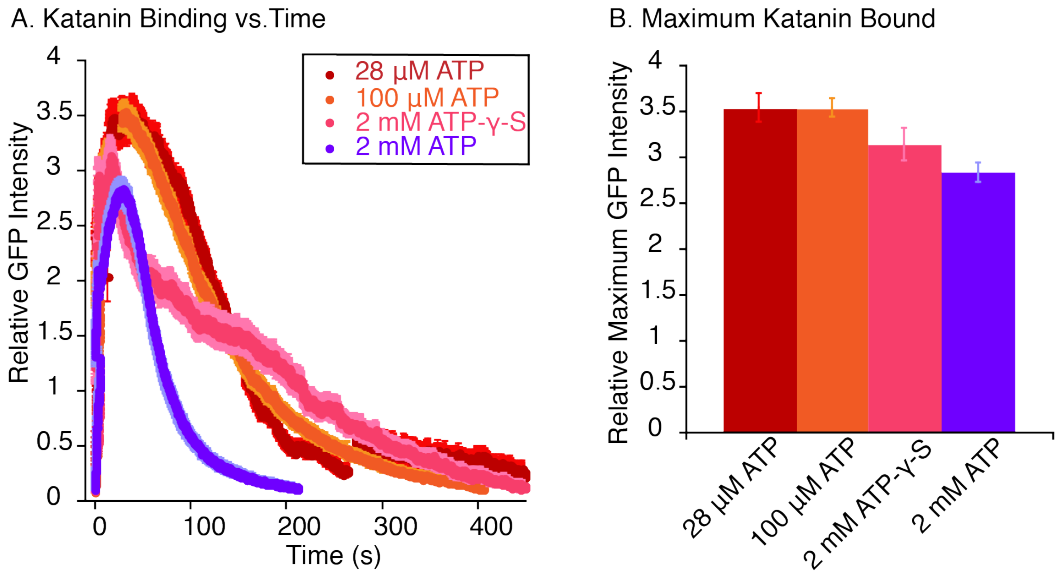

Figure 10. Quantification of Katanin Binding to Taxol-stabilized Microtubules with Low Concentration of ATP.

A) Total katanin bound to microtubules over time for each of the conditions. The first thirty seconds of each video was used as a control to make sure that nothing was binding to the microtubules before GFP-katanin was flown in. Katanin with: 28 µM ATP is red (N=39 in 2 different chambers); 100 µM ATP is orange (N=85 in 3 different chambers); 2 mM ATP-γ-S is pink (N=52 in 3 different chambers); and 2 mM ATP control is purple (N=102 in 3 different chambers). Microtubules were completely destroyed in 100 µM and 2 mM ATP chambers only. In chambers with 28 µM ATP and 2 mM ATP-γ-S, microtubules were not completely destroyed after looking through the chamber after imaging. The error bars are lighter versions of their marker colors and represent the SE. B) The maximum GFP intensity from A) was plotted in B) and the error bars represent the SE of that value.

2.3.4 Katanin Binding and Activity is Inhibited at High Concentrations of ATP

Previously, our lab identified that katanin severing and depolymerization activity is inhibited at high concentrations of ATP including 5 mM, 10 mM, and 20 mM (Fig. 5). However, we were interested in further investigating the mechanism of inhibition. We studied katanin activity on Taxol-stabilized microtubules in the presence of the same concentrations of ATP with our fluorescently-labeled katanin to understand if katanin was binding to the microtubules. Representative time series of show katanin binding is affected at high concentrations of ATP (Fig. 11A,B,C). We examined the rest of the chamber and microtubules remained in all conditions, indicating katanin activity was indeed inhibited.

The data was quantified as relative GFP intensity over time (Fig. 12A). We quantified the exponential decay phase of the data, that is, after maximum binding of GFP-katanin and fit the data to a single exponential decay (Eq. 1). Characteristic decay times were extracted and compared. Compared to the characteristic decay time of the 2 mM ATP control, all conditions with a higher concentration of ATP had significantly longer characteristic decay times. The characteristic decay time of the 2 mM ATP control is 46 ± 0.1 s. The characteristic decay times of 5, 10, and 20 mM ATP are 102 ± 0.5 s, 159 ± 0.2 s, and 210 ± 1.0 s, respectively. Clearly, as ATP concentration increases, characteristic decay time increases as well. This is further evidence that katanin activity on microtubules is decreasing as ATP concentration increases.

Compared to the 2 mM ATP control, there was significantly less katanin bound to microtubules at 5, 10, and 20 mM ATP. In addition, as ATP concentration increased, the amount of katanin bound to microtubules decreased. The relative maximum GFP intensity was extracted (Fig. 12B) and the same trend was observed. In the presence of 5 mM ATP, the relative maximum katanin bound was 1.6 ± 0.06 compared with 2.8 ± 0.1

for 2 mM ATP. Similarly, the relative maximum katanin bound was 1.2 ± 0.05 in the presence of 10 mM ATP. At 20 mM ATP, the relative maximum katanin bound was 0.2 ± 0.02, comparable to that of the no katanin control 0.01 ± 0.05. This data clearly identifies that an increase in ATP concentration leads to reduced binding of katain on microtubules and thus reduces katanin activity.

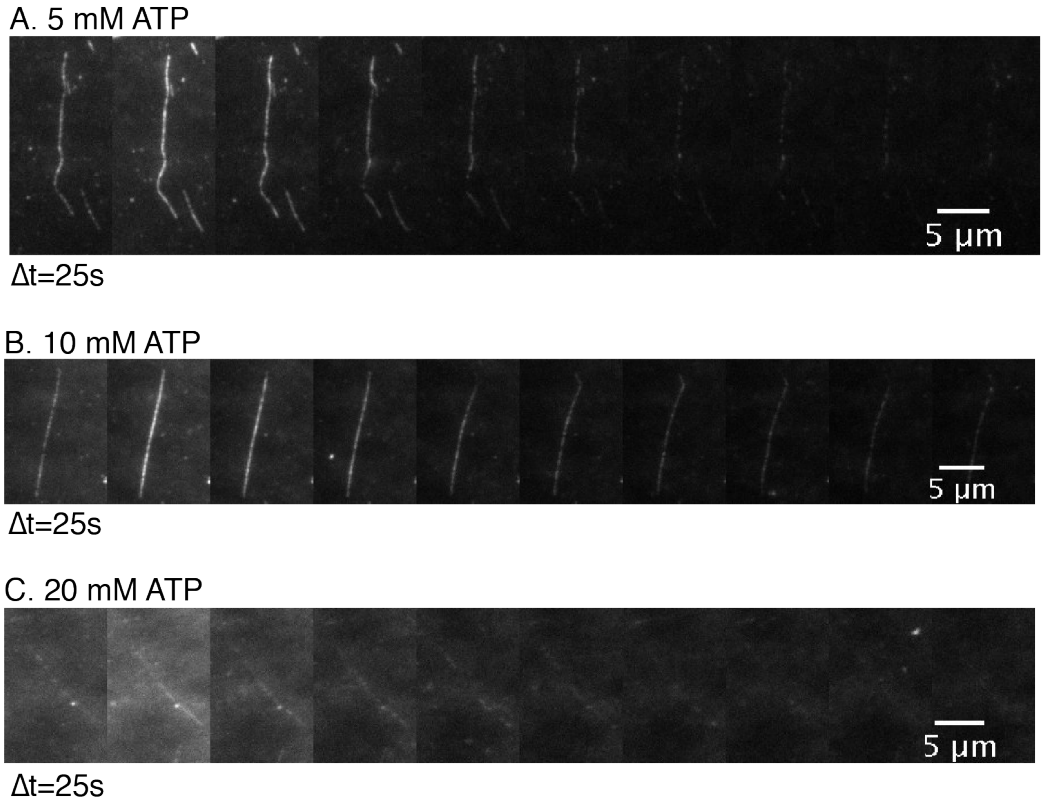

Figure 11. Representative Time Series of Inhibition of Katanin Binding and Severing on Taxol-stabilized Microtubules.
Time series representative of katanin on Taxol-stabilized microtubules in a severing assay with A) 5 mM ATP B) 10 mM ATP, or C) 20 mM ATP. Binding to microtubules decreases as the concentration of ATP increases. This inhibits katanin activity on microtubules, consistent with previous findings from our lab. The time between images is 25 seconds for each time series and all scale bars are 5 µm.

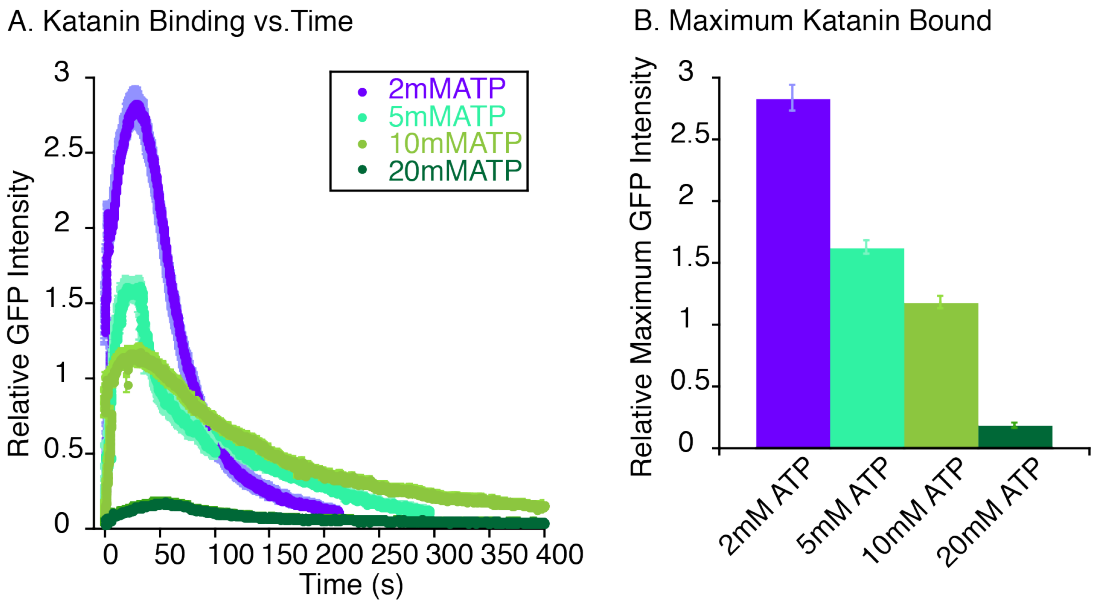

Figure 12. Quantification of Katanin Binding to Taxol-stabilized Microtubules with High Concentration of ATP.

A) Total katanin bound to microtubules over time for each of the conditions. The first thirty seconds of each video was used as a control to make sure that nothing was binding to the microtubules before GFP-katanin was flown in (not shown). Katanin with 5 mM ATP is light green (N=67 in 2 different chambers); 10 mM ATP is olive green (N=71 in 3 different chambers); 20 mM ATP is dark green (N=79 in 3 different chambers); and 2 mM ATP control is purple (N=102 in 3 different chambers). Only in chambers with 2 mM ATP were the microtubules completely destroyed. The error bars are a lighter version of the color of their markers and represent the SE. In the case of 20 mM ATP, error bars are so small that most are smaller than the marker itself. B) The relative maximum GFP from A) is plotted and the error bars are ± SE.

2.3.5 Mechanism is Conserved in *Xenopus* and Human Katanin p60

Our results show that the activity of katanin is dependent on the concentration of ATP. At low concentration of ATP or in the presence of the non-hydrolysable ATP homologue ATP-γ-S, there is microtubule depolymerization (Fig. 9A,B,C). However, at moderate concentrations of ATP, there are distinct severing events (Fig. 6B,C,D). At high concentrations of ATP, there is neither depolymerization nor severing because the binding of katanin is inhibited (Fig. 11 A,B,C). These results are consistent with our previous results with *X. laevis*-p60 without a GFP tag (Fig. 5). Our lab previously showed polymer loss of microtubules was dependent on ATP concentration and there is a depolymerization regime and a severing regime. This data coupled with the data shown here demonstrates that ATP-bound katanin binds to microtubules and is in fact leading to these regimes of depolymerization and severing. This is important evidence that will be useful in elucidating katanin's mechanism of depolymerization. It suggests ATP-binding may regulate the type of katanin activity exhibited on a microtubule. This may be important to the cell as the cell could regulate dynamic cellular processes by increasing or decreasing the local concentration of ATP.

2.4 Discussion

Katanin binding decreases at high concentrations of ATP (Fig. 12A). A couple of possibilities exist to explain this: 1) the motor is jammed with ATP, preventing hexamerization of katanin on the microtubule, 2) increasing the ionic strength of the chamber screens the interaction of katanin and the microtubule. First, we will discuss evidence for ATP jamming the motor. Crystal structures of katanin show there may be cycling of the hexamer between open spiral and closed ring where there is 5 ATP and 6 ATP molecules bound, respectively (Zehr et al., 2017). It was proposed that this cycling between conformations may provide the power stroke necessary for microtubule severing. High concentrations of ATP may encourage all katanin monomers to bind to ATP causing katanin to hexamerize in solution in the closed ring conformation. However, if hexamerization must occur on the carboxy-terminal tail in the open spiral conformation then these high concentrations of ATP would encourage hexamerization before docking and thus, katanin would be left in the closed ring position. It is possible that in this conformation, katanin would not be able to bind to the carboxy-terminal tail.

There is also evidence that the ionic strength of the buffer affects binding. ATP-Mg^{2+} is high in magnesium ions, which are good for screening. For every ATP molecule, there is one magnesium counterion with a valence of two. Therefore, as we increase the ATP concentration, we are also increasing the ionic strength of the buffer. Previous results have shown that the ionic strength of the buffer does affect the binding and diffusion of individual katanin monomers (Eckert et al., 2012). In that study, the ionic strength of their base buffer (50 mM HEPES) was similar to ours (20 mM HEPES), and they added NaCl (valence of +1) to 80 mM, 160 mM, or 300 mM. At 80 mM NaCl, they saw a typical landing rate for katanin in your microscopic assays, which decreased as the ionic strength increased. The ionic strength of their buffer (50 mM HEPES) with 80

mM NaCl is far higher than our buffer (20 mM HEPES) with 20 mM ATP-Mg^{2+}, implying that the ionic strength in our assays is not high enough to be the cause of the reduced dissociation rate. A number of cytoskeletal enzymes have an ATPase cycle where the affinity of the motor is lower in the ATP-state, including dynein for microtubules and myosin for actin filaments. It is possible that katanin also has a lower affinity with ATP at saturating concentrations.

As expected, katanin activity decreases when katanin binding is decreased. Katanin is a cooperative enzyme, and its activity depends on the concentration of hexamers present on the filaments. This is consistent with all the data collected thus far. There seems to be a critical concentration for ATP switching the enzyme from depolymerizing to severing. Additionally, when finding the working concentration of the enzyme in the beginning of every assay, the enzyme appears to have an on/off switch for severing very quickly upon increasing the concentration of katanin. There appears to be a "critical concentration" at which katanin severs. In the cell, this would more likely look like an "optimal ratio" of katanin to ATP. This may be evidence for the jammed motor hypothesis, however, it is more than likely that multiple methods of regulating katanin are employed.

CHAPTER 3

KATANIN DEPOLYMERIZES TAIL-LESS MICROTUBULES

3.1 Introduction

The cell is dynamic and is constantly being remodeled to undergo different cellular processes. Katanin is an essential regulator of the microtubule cytoskeleton by helping to remodel microtubule networks to meet the demands of the cell. Because katanin is a catastrophe factor, it was originally and is still often thought of as quickly destroying microtubules. Indeed, katanin can remove tubulin dimers causing microtubule catastrophe. However, a different purpose for katanin severing was recently found. In addition to destroying the entire polymer, katanin severing can also create short microtubule seeds for new growth (Roll-Mecak & Vale, 2006; Srayko, Buster, Bazirgan, Mcnally, & Mains, 2000). This new understanding of katanin severing activity on microtubules helped researchers better understand katanin's role in many cellular processes.

We have some understanding about how severing happens. To sever microtubules, katanin uses ATP to oligomerize into a hexamer and then disassembles microtubules by threading the carboxy-terminal tail (CTT) of tubulin through its pore (Roll-Mecak & Vale, 2008). Our lab showed that katanin binds to free-dimers of tubulin or CTTs, which turns off microtubule severing (Bailey et al., 2015). Clearly, katanin has a preference for CTTs of free tubulin. In addition, previous research also showed that subtilisin-treated microtubules, which lack the CTTs of tubulin, were safe from severing (McNally & Vale, 1993). These data all imply that the CTT is the essential target for katanin severing.

However, several groups have noticed that katanin has the ability to depolymerize microtubules in addition to severing (Diaz-Valencia et al., 2011; McNally &

Vale, 1993; Zhang et al., 2011). Depolymerization may be especially important in regulating microtubule length, such as at the cortex in interphase cells and kinetochore fibers in mitosis. Spastin, fidgetin and katanin are all required for proper chromosome segregation during the anaphase of mitosis (Zhang et al., 2007). Katanin stimulates plus-end depolymerization at the kinetochores of spindles by uncapping microtubules (Zhang et al., 2007). This stimulates chromosome-attached microtubules to depolymerize at their plus ends, a type of motility termed Pacman. It is thought that kinesin-13 is a primary depolymerizer of microtubule plus-ends in mitosis, but it is possible katanin plays more of a role active role in aiding kinesin-13 in depolymerizing microtubules in addition to uncapping microtubules.

To depolymerize, katanin acts at microtubule ends, depolymerizing microtubules in an ATP-dependent manner (Diaz-Valencia et al., 2011; Zhang et al., 2011). This type of katanin activity may be distinct from severing because it occurs at the ends of microtubules. Likewise, the mechanism is likely also different. We use in vitro reconstitution assays to probe whether katanin targets microtubules that lack the CTT of tubulin and altered the nucleotide state bound to katanin. We provide evidence that the CTT is not necessary for depolymerization, as it is in severing.

3.2 Methods

3.2.1 Protein Purification

Our lab received the *X. laevis* katanin construct from the Heald lab. It has a maltose binding protein on the N-terminus for purification and is a full-length katanin p60. Megan Bailey purified the katanin with a maltose binding protein and chromatography system. After transforming the plasmid into BL21 competent *E.coli* cells (New England BioLabs), she grew the culture in a 5 ml LB starter culture overnight. She grew a larger culture at 37°C until it reached an OD of 0.8 and then induced with IPTG. The culture was allowed to shake at 16°C for 16 hours. Cells were pelleted then lysed in resuspension buffer (20 mM Hepes pH 7.7, 250 mM NaCl, 0.5 mM BME, 10% glycerol, 0.25 mM ATP) via sonication. The lysate was mixed with amylose resin beads on a rocker for 1.5 hours. The mixture was passed through a chromatography column to collect maltose-bound katanin and washed with 20 ml of resuspension buffer. The protein was eluted in elution buffer (20 mM Hepes pH 7.7, 250 mM NaCl, 0.5 mM BME, 10% glycerol, 0.25 mM ATP, 10 mM maltose) and the concentration of protein was determined via Bradford assay. The protein was used the same day and later, a gel was run to check protein purity.

3.2.2 Taxol-stabilized Microtubule Polymerization

Megan Bailey made Taxol-stabilized microtubules by combining a 1:3-1:20 ratio of labeled rhodamine tubulin (Cytoskeleton Inc.) or homemade Dylight 649 (Thermo Scientific) tubulin with purified unlabeled tubulin made from porcine brains in house using the method described in (Peloquin et al., 2005). She resuspended both the unlabeled and labeled tubulin in PEM-100 (100 mM K-Pipes, pH 6.8, 2 mM $MgSO_4$, 2 mM EGTA) to a concentration of 5 mg/mL (45.5 μM) and incubated it on ice for 10 minutes. We combined the labeled and unlabeled tubulin and centrifuged at 366,000xg

at 4°C for 10 minutes to remove aggregated or insoluble tubulin. 1 mM GTP was added to the tubulin and incubated at 37°C for 20 minutes to polymerize the microtubules. Then, 50 μM Taxol was added and incubated for 20 minutes at 37°C to stabilize the microtubules. Microtubules were centrifuged at 16,200xg at 27°C for 10 minutes to remove tubulin aggregates and further purify microtubules. The microtubule pellet was resuspended in PEM-100 and 50 μM Taxol to further stabilize microtubules.

3.2.3 Subtilisin-treated Taxol-stabilized Microtubule Polymerization

Microtubules lacking the carboxy-terminal tails were made by treating microtubules with subtilisin. After polymerizing Taxol microtubules, we incubated them with 100 μg/mL subtilisin for 45 minutes. The reaction was stopped using 2 mM PMSF. We further removed the subtilisin by centrifuging the microtubules for 30 minutes at 16,200xg 27°C. We resuspended the pellet in PEM-100 and 50 μM Taxol.

3.2.4 In vitro assays

Megan Bailey collected the data using *in vitro* katanin severing assays. Coverslips were cleaned and silanized with 2% dimethyldichlorosilane (GE Healthcare) to block the surface and prevent proteins from sticking to the surface of the coverslips. Silanized coverslips are assembled onto glass slides using double-stick tape. This provides space in between the slides to flow buffers and proteins and keeps the coverslip stuck to the slide. Then, she flowed 10 ul washes as follows with five minute incubation periods between. First, she flowed in an antibody to tubulin, MAB1864 (Sigma) at 2% (w/v) in Katanin Activity Buffer (20 mM Hepes pH 7.7, 10% glycerol, 2 mM $MgCl_2$) to stick the microtubules to the surface. Then, she flowed in 5% (w/v) Pluronic F-127 in Katanin Activity Buffer (20 mM Hepes pH 7.7, 10% glycerol, 2 mM $MgCl_2$) to block the surface. Next, she flowed in a 1:100 dilution of labeled microtubules

to stick to the antibody surface. Finally, she washed the chamber to flow out excess unbound microtubules with wash buffer (20 mM Hepes pH 7.7, 10% glycerol, 2 mM $MgCl_2$, 2 mM ATP, 0.025 mg/mL BSA, 0.05% F-127, 10 mM DTT, 15 mg/mL glucose, 0.15 mg/mL catalase, 0.05 mg/mL glucose oxidase).

3.2.5 Microscopy

Our lab houses a Nikon Ti-E microscopy with a 60x objective (NA 1.49) which was used coupled with a 4x expander, and an iXon EM-CCD camera. The microscope has an epi-fluorescence light source which we used to image microtubules. The chamber was imaged prior to adding katanin to check the microtubules and to make sure our imaging conditions did not damage the microtubules. We captured images of fluorescent microtubules every 5 s with shuttering between. This ensured that photodegradation did not occur. We imaged for 3 minutes before flowing in the experimental buffer to make sure the microtubules were not falling apart due to something other than katanin. The experimental buffer contained either no katanin or 250 nM katanin (wild type katanin or mutant E306Q katanin). If a different nucleotide was being tested, the enzymatic mix was made without ATP and another nucleotide was substituted in instead (5 mM AMPPNP or 5 mM ADP). Movies were taken at 5 second intervals for 10 minutes.

3.2.6 Loss of Polymer Data Analysis

Megan Bailey completed the loss of polymer analysis in ImageJ as previously described (Bailey et al., 2015). Time series data were imported into ImageJ as nd2 files. She used the line tool to draw a segmented line, 3 pixels wide, over the length of the microtubule. We used the macro “measure stacks” to measure the mean intensity of the line for each frame of the movie. The same line was moved to a location without

microtubules to measure the background intensity near the microtubules. The intensity was normalized by dividing the intensity by the background ($I_{measured}/I_{BG}$) and then subtracted from 1 so that all the data sets started at a normalized intensity of 1. The individual, normalized microtubule intensity data were then averaged together and the error bars represent the standard error of the mean. The data was either fit to a linear approximation (chambers with no katanin) or an exponential decay (chambers with katanin).

3.2.7 Depolymerization Speed Analysis

Depolymerization speed analysis was performed in ImageJ. I used the line tool to draw a 3-pixel wide line over the microtubule and used the "Reslice" function to make a kymograph with distance on the x axis and time on the y axis. The microtubule polymer loss has good signal to noise in kymographs making it relatively easy to distinguish the microtubule from the background. Using the box tool, we measured the number of pixels of the height and width of the box corresponding to the time and distance of depolymerization, respectively. The pixel conversion in the x-axis is 67.5 nm per pixel. The pixel conversion in the y-axis is 5 s per pixel. We calculated the depolymerization speed in nm/s by dividing the distance by the time. Each end was measured separately and averaged. The data was fit to a rising exponential decay function to determine the best fit using least squares fitting routine in KaliedaGraph.

3.3 Results

3.3.1 Katanin Depolymerizes Tail-less Microtubules

We are interested in understanding the mechanism of katanin depolymerization on microtubules and how it may be different from the mechanism of severing. First, we must quantify total loss of polymer to then distinguish microtubule severing from depolymerization. We show that wild type katanin is able to sever Taxol-stabilized microtubules but not subtilisin-treated microtubules (Fig. 13A). I hand-counted the number of severing events. The number of severing events on microtubules was 94 and 0, on Taxol-stabilized microtubules and subtilisin microtubules, respectively. We also quantified total katanin activity by plotting total loss of polymer over time (Fig. 13B). Taxol and subtilisin-treated microtubules alone did not lose significant amounts of polymer. This is an important control that shows the microtubules do not fall apart over time. Microtubules alone were best fit was to a linear approximation:

$$\mathbf{I(t)=I_{max}(1-(t/\tau))\ (Eq.\ 2)}$$

where I is intensity as a function of time, t, I_{max} is the maximum intensity, and τ is the characteristic decay constant. The characteristic decay time for Taxol microtubules alone is 3,220 ± 80 s and is 22,000 ± 5,000 s for subtilisin microtubules alone. These values are very large and the data suggests tail-less microtubules are more stable than Taxol microtubules. This is consistent with previous work (Bhattacharyya et al., 1985; Maccioni, Serrano, Avila, & Cann, 1986; Serrano, Valencia, Caballero, & Avila, 1986). Measuring microtubule fluorescence over time is an important control, however, we are interested in the effect of katanin on these microtubules.

Thus, we also quantified microtubule loss in the presence of katanin. In the presence of katanin, Taxol-stabilized microtubules and subtilisin microtubules were

destroyed (Fig. 13B). Loss of polymer data in the presence of katanin was fit with exponential decay parameters for a single exponential similar to (Eq. 1):

$$\mathbf{I(t)=I_{max}exp(-t/\tau)+I_{\infty}\ (Eq.\ 3)}$$

where I is intensity as a function of time, t, and τ is the characteristic decay constant. I_{max} is the maximum amplitude and I_{∞} represents the final intensity of microtubules not fully degraded by katanin. From this equation, we extracted characteristic decay times. The characteristic decay time for katanin on Taxol microtubules and subtilisin microtubules is 97 ± 2 s and 105 ± 8 s, respectively (Fig. 13C). Surprisingly, these quantitative results of the rate of the loss of polymer are not significantly different. This suggests the rate of katanin activity on microtubules with and without tails is similar. Yet, we observe that the mechanism of the loss of polymer is distinct for subtilisin-treated microtubules and Taxol microtubules. Specifically, in control microtubules, the filaments are severed, but subtilisin-treated microtubules are only depolymerized (Fig. 13A, 14A). To further investigate katanin activity, we also quantified the percent total loss of polymer (Fig. 13D). Wild type katanin could completely destroy Taxol microtubules but destroyed only 50 ± 10% of subtilisin-treated microtubules. Although characteristic decay times are the same, this evidence suggests katanin is acting on subtilisin microtubules in a way that is distinct from severing.

Our metric to measure the loss of polymer does not distinguish severing from depolymerization. Thus, we used kymographs (space-time projections) to measure depolymerization from the ends of microtubules. We show that microtubules alone do not depolymerize (Fig. 14A). However, upon the addition of katanin, both control and subtilisin-treated microtubules are depolymerized. We quantified the depolymerization speeds using cumulative distributions (Fig. 14B). Data with katanin was fit with a single rising decay:

CDF(v)=1-Aexp(-v/v*) (Eq. 3)

where the cumulative distribution function (CDF) is a function of depolymerization velocity, v, v* is the characteristic velocity of the rising decay, and A is the amplitude of the exponential. We compared the characteristic speeds of depolymerization we extracted from this fit (Fig. 14C). In the presence of katanin, Taxol-stabilized microtubules and subtilisin microtubules exhibited similar characteristic velocities of 2.3 ± 0.02 nm/s and 1.89 ± 0.07 nm/s, respectively.

We also quantified the percent of microtubule ends that displayed depolymerization (Fig. 14D). Only 31 ± 6% of Taxol-stabilized microtubule ends and 10 ± 6% of subtilisin microtubule ends depolymerized on their own. In comparison, 96 ± 2% Taxol-stabilized microtubule ends and 91 ± 5% of all subtilisin microtubule ends were depolymerized in the presence of katanin. These values are within statistical significance and therefore suggest katanin can depolymerize control microtubules and subtilisin microtubules to the same degree. Our research suggests katanin does not require the CTT to depolymerize microtubules, which is evidence for a mechanism that is different than that of severing.

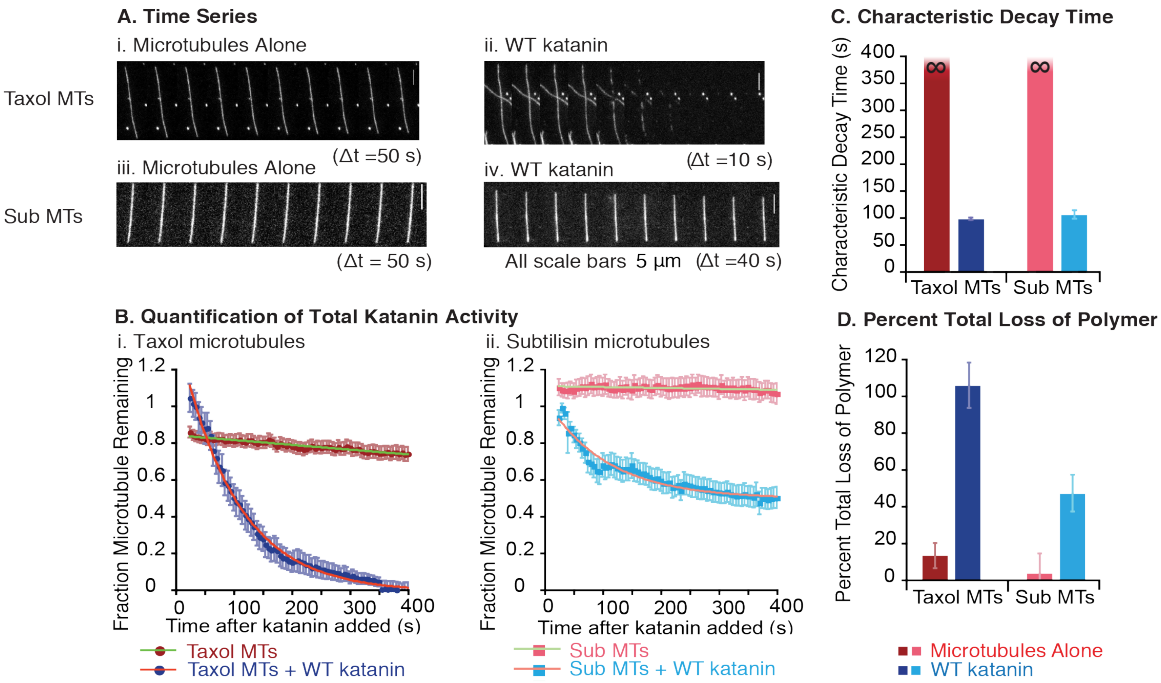

Figure 13. Wild Type Katanin Total Loss of Polymer on Taxol and Subtilisin Microtubules.

(A) Time series representative of microtubules over time in a severing assay. (i) Taxol-stabilized microtubules alone, without katanin, or (ii) with katanin. (iii) Taxol-stabilized subtilisin-treated microtubules alone, without katanin, or (iv) with katanin. The time between images is as stated below each time series and all the scale bars are 5 µm. (B) Quantification of the total loss of microtubule polymer over time for each condition. (i) Taxol microtubules without katanin (dark red circles, N=33 in 6 different chambers) and Taxol microtubules with katanin (dark blue circles, N=51 in 8 different chambers). (ii) Subtilisin-treated microtubules without katanin (light red squares, N=30 in 3 different chambers) and subtilisin-treated microtubules with katanin (light blue squares, N=35 in 9 different chambers). Error bars represent the standard error of the mean. Data without katanin were fit with a linear approximation to an exponential decay (Eq. 2, green lines). Data with katanin present were fit with an exponential decay (Eq. 3, red lines). All fit parameters can be found in Appendix A. (C) Characteristic decay times from (B) are plotted as bars for Taxol microtubules without katanin (dark red), Taxol microtubules with katanin (dark blue), subtilisin-treated microtubules without katanin (light red), and subtilisin-treated microtubules with katanin (light blue). Error bars represent the uncertainty of the fit parameters from least-squares fitting. (D) The fraction of the initial microtubule polymer left after 10 minutes of experiment from (B) are plotted as bar graphs for Taxol microtubules without katanin (dark red), Taxol microtubules with katanin (dark blue), subtilisin-treated microtubules without katanin (light red), and subtilisin-treated microtubules with katanin (light blue). The error bars represent the uncertainty of the fit parameters from least-squares fitting.

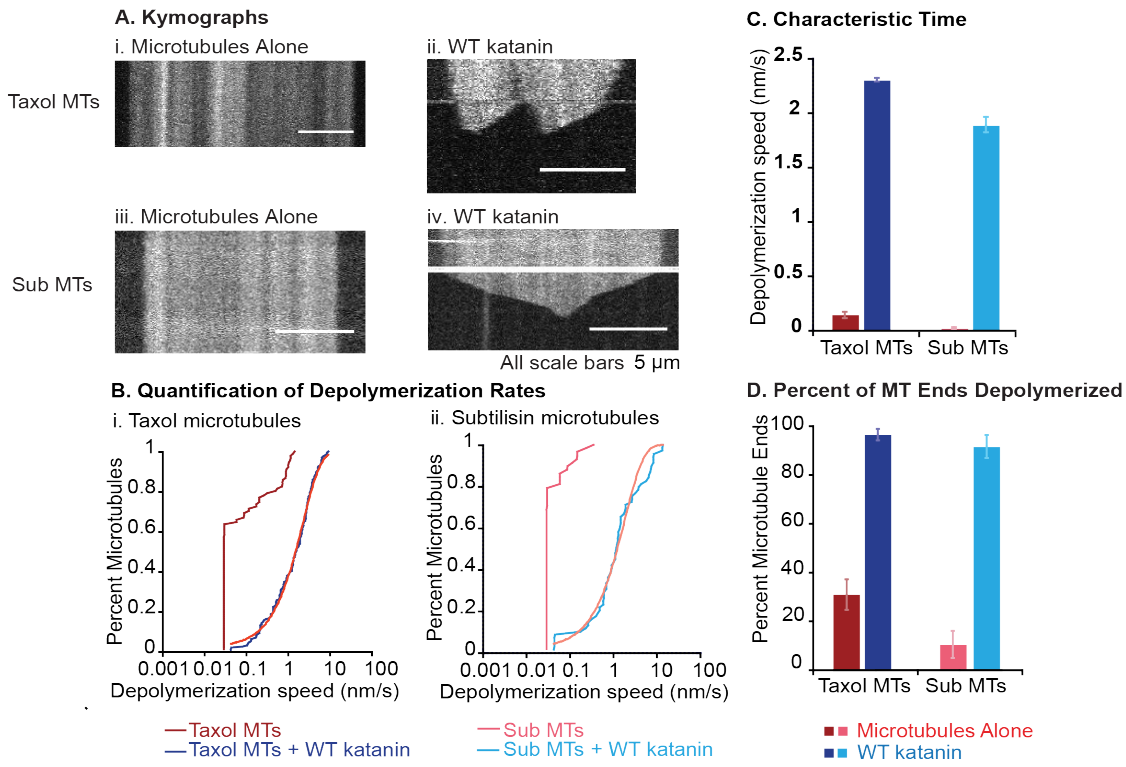

Figure 14. Wild Type Katanin Depolymerization on Taxol and Subtilisin Microtubules. (A) Kymographs representative of microtubule severing and depolymerization. (i) Taxol-stabilized microtubule alone, (ii) Taxol-stabilized microtubules with katanin and ATP, (iii) subtilisin microtubules alone, and (iv), subtilisin microtubules with katanin and ATP. The horizontal white lines seen in the kymographs denote when the room lights were turned on to flow katanin into the flow chamber. The total height of the kymographs represent 600 s. Horizontal scale bars represent 5 µm. (B) Cumulative distributions of the depolymerization speeds of (i) Taxol and (ii) subtilisin microtubules with and without katanin. (i) Taxol-stabilized microtubules without katanin (dark red line, N=54 in 7 different chambers) and Taxol-stabilized microtubules with katanin (dark blue line, N=66 in 10 different chambers). (ii) Subtilisin microtubules without katanin (light red line, N=30 in 3 different chambers) and subtilisin microtubules with katanin (light blue line, N=35 in 9 different chambers). Data was fit with a single rising decay (Eq. 4) (C) Quantification of characteristic depolymerization times from (B) are plotted as bars for Taxol microtubules without katanin (dark red), Taxol microtubules with katanin (dark blue), subtilisin-treated microtubules without katanin (light red), and subtilisin-treated microtubules with katanin (light blue). The error bars are the error associated with the rising decay time of the fits in (B). (D) Percent of microtubules depolymerized (considered any value above 0.1125 nm/s). This value was determined based on the smallest speed of depolymerization that can be calculated with one pixel wide measurement using the box tool. Error bars represent the standard error of proportion.

3.3.2 Enzymatically Dead Katanin Depolymerizes Microtubules

We seek to better understand the mechanism of microtubule depolymerization by katanin. Therefore, we also assessed the activity of the enzymatically dead Walker B mutant katanin on microtubules. The *X. laevis* E306Q mutant is deficient in ATP-hydrolysis, and therefore cannot sever microtubules (Loughlin et al., 2011). However, the ability of the *X. laevis* Walker B mutant to depolymerize microtubules has not yet been assessed. Therefore, we characterized the activity of the Walker B mutant *X. laevis* p60 on both Taxol-stabilized and subtilisin microtubules.

Time series of microtubules show that the Walker B mutant is unable to sever any type of microtubule, as expected (Fig. 15A). To verify this, we recorded the total number of severing events by hand. There was a total of 4 severing events on Taxol-stabilized microtubules and 0 severing events on subtilisin microtubules. However, we noticed significant microtubule loss when we quantified the total loss of polymer (Fig. 15B). Since the Walker B mutant katanin was unable to sever microtubules, the loss of polymer is due to endwise depolymerization. We fit the data to a single exponential decay (Eq. 3) to extract the characteristic decay times. The characteristic decay time of Taxol-stabilized microtubules and subtilisin microtubules in the presence of the Walker B mutant is 290 ± 20s and 240 ± 40s, respectively (Fig. 15C). This suggests the rate of activity of the Walker B katanin is similar on both microtubules with and without CTTs. Although the characteristic decay times are similar on both Taxol-stabilized and subtilisin microtubules, the total loss of polymer is significantly different. The total loss of polymer in the presence of the Walker B mutant katanin was 37 ± 7% for Taxol-stabilized microtubules but only 9 ± 6% subtilisin-treated microtubules (Fig. 15D). This suggests that the degree to which microtubules are degraded by the Walker B mutant katanin is, in fact, dependent on the CTT.

We continued to investigate the hypothesis that the Walker B mutant katanin could depolymerize, although not sever, microtubules. Kymographs of Taxol-stabilized and subtilisin microtubules show slight loss of polymer from both ends (Fig. 16A). We used a cumulative distribution function to quantify the depolymerization speeds (Fig. 4B). We fit the data to the single rising decay (Eq. 4) to extract the characteristic times. The characteristic speed of the Walker B mutant katanin is 0.43 ± 0.02 nm/s on Taxol-stabilized microtubules and 0.31 ± 0.02 nm/s on subtilisin microtubules (Fig. 16C). These values are significantly lower than the characteristic depolymerization speeds for wild type katanin (Fig. 16C). We also examined the percentage of filaments that depolymerized and find 57 ± 6% of Taxol-stabilized microtubules depolymerized and 55 ± 9% of subtilisin microtubules depolymerized (Fig. 16D). For each type of microtubule, the wild type katanin was more efficient at depolymerizing microtubules (Fig. 16D), but the effect was negated by the ATP-deficient mutation. This implies that the depolymerization depends on the ability to use ATP and the availability of tubulin CTTs.

3.3.3 Activity of ADP-bound Wild Type Katanin is Similar to Enzymatically Dead Mutant

It has long been known that katanin's ability to sever microtubules is strictly nucleotide dependent and requiring ATP and a functional AAA enzyme domain (F. J. McNally & Vale, 1993). Our lab has shown that both severing and depolymerization are ATP-dependent (Diaz-Valencia et al., 2011).

We tested the ability of wild type katanin to sever and depolymerize in the presence of ADP. We expected that the ADP-bound wild type katanin would be similar to the enzymatically dead mutant (E309Q) in both lacking of microtubule severing and reduced depolymerization of microtubules. As expected, we observed a lack of severing

by wild type katanin when ADP was present consistent with our prior results and those from other groups (Johjima et al., 2015) (Fig. 15A). We quantified the total loss of polymer fit the data to a single exponential decay (Eq. 3), and the characteristic times were extracted (Figs. 15B). The characteristic decay times in the presence of ADP-bound wild type katanin on Taxol-stabilized microtubules is 560 ± 70 s and 410 ± 40 s on subtilisin microtubules.

The ADP-bound katanin and Walker B mutant katanin was within statistical significance for all time points during total loss of polymer of Taxol-stabilized microtubules. Data were similar but statistically different for the ADP-bound katanin and Walker B mutant katanin on subtilisin microtubules. The data from the characteristic decay times suggests that the loss of polymer due to depolymerization depends more on the enzymatic activity of katanin than the presence of the CTT. We next compared the total loss of polymer (Fig. 15D). We found that the total loss of polymer was higher on Taxol-stabilized microtubules 50 ± 10% than subtilisin-treated microtubules 37 ± 7%, but they were within uncertainty of each other.

We quantified the depolymerization rates for wild type katanin in the presence of ADP using kymographs (Fig. 16A). The were plotted in a cumulative distribution and fit to a rising exponential decay (Eq. 4) (Fig. 16B). The characteristic depolymerization speeds were 1.5 ± 0.03 nm/s for Taxol-stabilized microtubules and 0.4 ± 0.02 nm/s for subtilisin-treated microtubules (Fig. 16C). We also quantified the percentage of microtubule ends that displayed depolymerization and found that 94 ± 4% of Taxol-stabilized microtubule ends were depolymerized with ADP-bound wild type katanin, and this value is not statistically different from ATP-bound wild type katanin. For subtilisin-treated microtubules, 76 ± 9% were depolymerized with ADP-bound katanin.

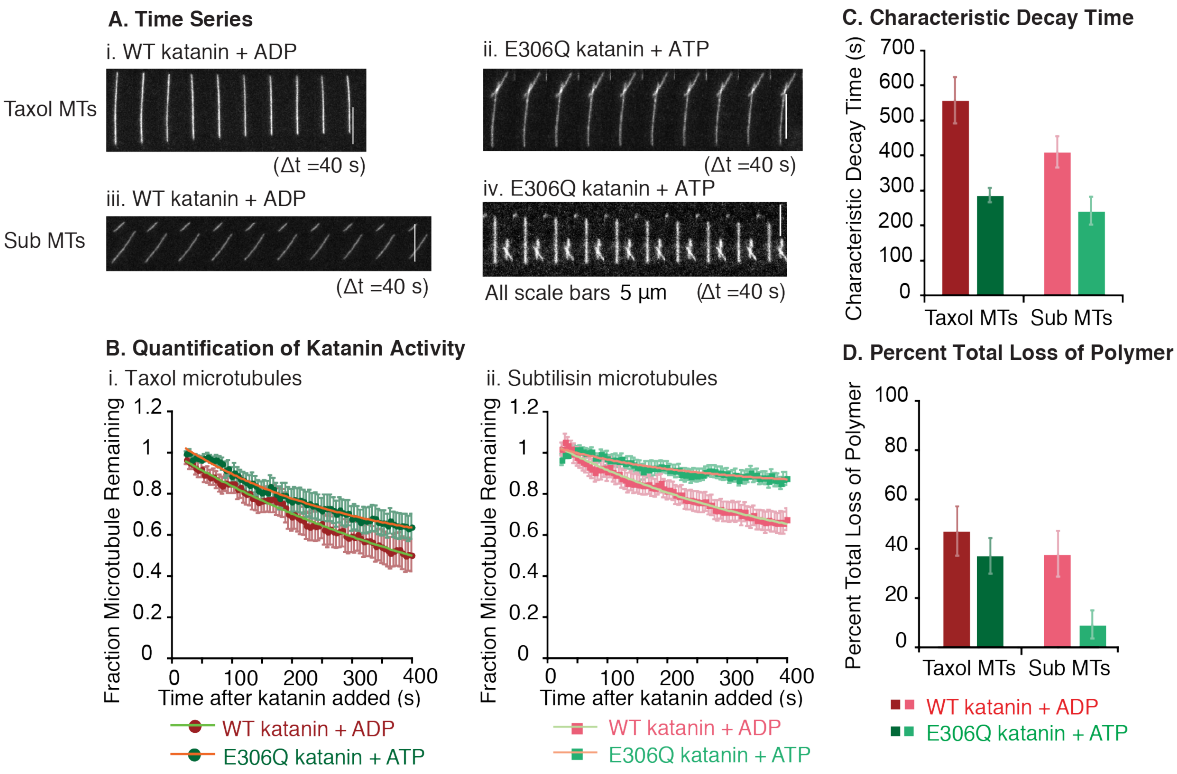

Figure 15. ADP-bound Wild Type Katanin and Enzymatically Dead Katanin (E309Q) have Similar Activity.

(A) Time series representative of a severing assay experimental parameters. (i) Taxol-stabilized microtubules in the presence of katanin with ADP, and (ii) Taxol microtubules in the presence of enzymatically dead mutant (E306Q) katanin with ATP. (iii) Subtilisin-treated microtubules in the presence of katanin with ADP (iv) Subtilisin-treated microtubules in the presence of E306Q katanin with ATP. The time between images is as stated below each time series and all the scale bars are all 5 µm. Neither the ADP-bound katanin nor the E306Q katanin, unable to hydrolyze ATP, was able to sever microtubules, but both displayed some depolymerization. (B) Quantification of total loss of polymer for (i) Taxol-stabilized microtubules and (ii) subtilisin microtubules. (i) Taxol-stabilized microtubules with wild type katanin and ADP (dark red circles, N=30 in 6 different chambers) and Taxol-stabilized microtubules with E306Q katanin with ATP (dark green circles, N=66 in 9 different chambers). (ii) Subtilisin microtubules with wild type katanin and ADP (light red squares, N=24 in 4 different chambers) and subtilisin microtubules with mutant katanin E306Q with ATP (light green squares, N=33 in 5 different chambers). Error bars represent the standard error of the mean. Data was fit with an exponential decay (Eq. 3). (C) Quantification of the characteristic decay times of exponential decay fits. (D) Percent total loss of polymer of the different conditions. The error bars are the uncertainty given from the least squares fitting routine.

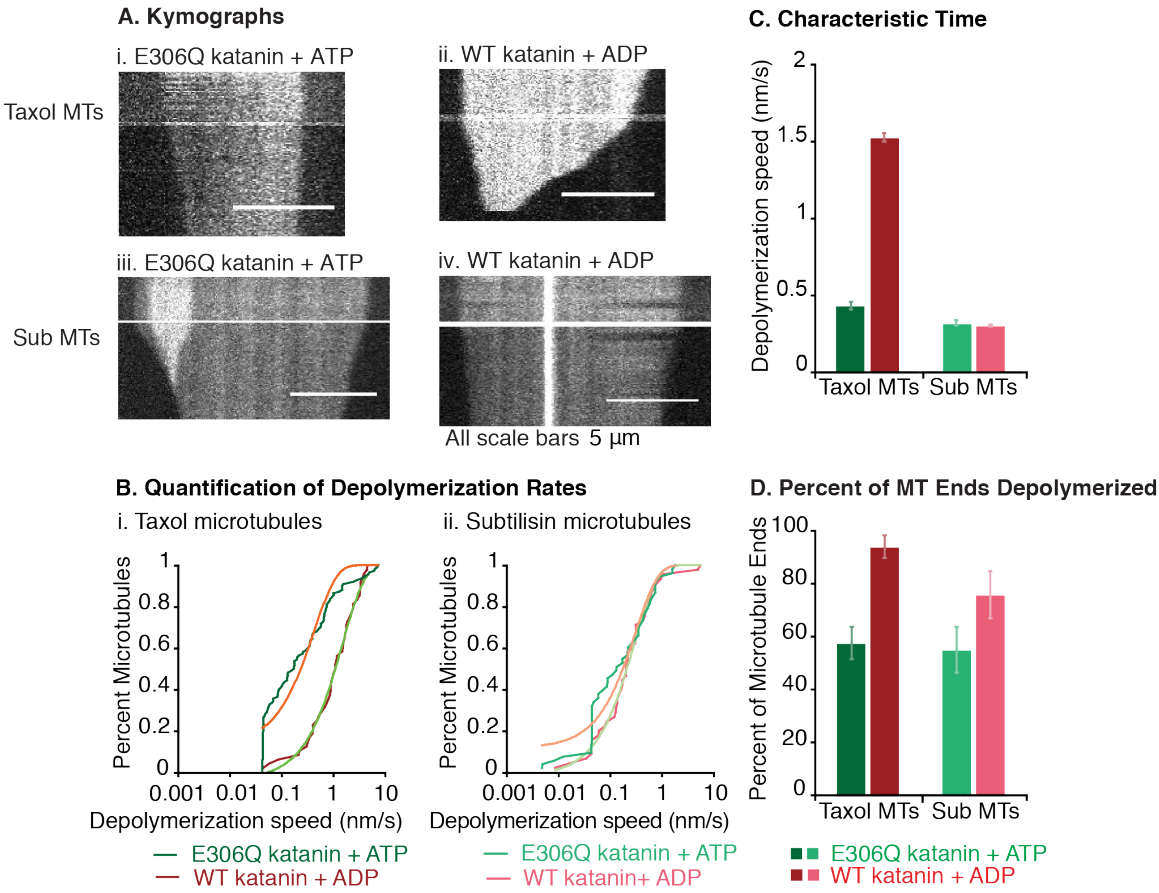

Figure 16. ADP-bound Katanin and Enzymatically Dead Katanin Depolymerize Similarly. (A) Kymographs representative of microtubule depolymerization. (i) Taxol microtubule with ADP-bound katanin and (ii) Taxol-stabilized microtubules with E306Q katanin. (iii) Subtilisin microtubules with ADP-bound katanin and (iv) subtilisin microtubules and E306Q katanin. The horizontal white line is when the lights were turned on to flow katanin into the flow chamber. The time is 600 s from the top of the kymograph to the bottom and all the scale bars are 5 µm. Movies were taken at 5 second intervals for 10 minutes. Each pixel is 5 seconds in the x direction and 67.5 nm in the y direction. (B) Cumulative distribution of the depolymerization speeds of (i) Taxol and (ii) subtilisin microtubules with either ADP-bound katanin or E306Q katanin. Taxol microtubules with ADP-bound katanin (dark red line, N=30 in 6 different chambers) and Taxol microtubules and E306Q katanin (dark green line, N=66 in 9 different chambers). (iii) Subtilisin microtubules with ADP-bound katanin (light red line, N=24 in 4 different chambers) and (iv) subtilisin microtubules with E306Q katanin (light green line, N=33 in 5 different chambers). Data was fit with a single rising decay (Eq. 4) (shown) (C) Quantification of characteristic depolymerization times for all conditions. The error bars are the error associated with the rising decay time of the fits in (B). (D) Percent of microtubules depolymerized (considered any value above 0.1125 nm/s). This value was determined based on the smallest speed of depolymerization that can be calculated with one pixel wide measurement using the box tool. Error bars represent the standard error of proportion.

3.3.4 AMPPNP is a Modest Inhibitor

We imaged wild type katanin in either the presence of ATP (Fig. 13,14) or AMPPNP and observed katanin was capable of severing (Fig. 17A). The total number of severing events of wild type *X. laevis* katanin on Taxol stabilized microtubules was 94 events in the presence of ATP and 88 events in the presence of AMMPNP over the observation time, so the ability to cause breaks was similar. We quantified the total loss of polymer over time and fit the data to an exponential decay (Eq. 3) (Fig. 17B). Although AMPPNP was a useable nucleotide for severing Taxol microtubules, the efficiency was reduced resulting in a longer decay time for AMPPNP (330 ± 30 s) compared to ATP (97 ± 2 s). We further quantified the total loss of polymer over the observation time for ATP and AMPPNP on Taxol microtubules (Fig. 17D). We observed that wild type katanin degraded 106 ± 9% of Taxol-stabilized microtubules in the presence of ATP but only 75 ± 6% of Taxol-stabilized microtubules in the presence of AMPPNP. Thus, the AMPPNP is not as good an energy course as ATP for loss of polymer in total, including severing and depolymerization.

We also measured the ability of wild type katanin to sever or destroy polymer on subtilisin microtubules in the presence of AMPPNP. Zero severing events were observed with ATP, and only 2 events were observed in the presence of AMPPNP. Loss of polymer data was fit to an exponential decay (Eq. 3) (Fig. 17B) and the characteristic decay times were quantified to reveal 105 ± 8 s with ATP and 360 ± 20 s with AMPPNP (Fig. 17C). On the other hand, subtilisin microtubules were unaffected by total loss of polymer upon changing nucleotide conditions. Wild type katanin degraded 47 ± 7% of subtilisin microtubules in the presence of ATP and 53 ± 5% in the presence of AMPPNP. Since depolymerization is the only mechanism available to account for the loss of polymer on the subtilisin microtubules, this suggests AMPPNP does not inhibit

depolymerization. Comparing the subtilisin-treated microtubules to Taxol microtubules, we observe that the characteristic loss of polymer depends more on the presence of the nucleotide than the presence of the carboxy-terminal tail. Indeed, the main difference between the Taxol and subtilisin microtubules is the overall loss of polymer, which is always higher for Taxol microtubules because those microtubules allow severing to occur in addition to depolymerization.

Thus, we quantified characteristic depolymerization rates to further tease out the differences between severing and depolymerization in the different nucleotide states by quantifying the depolymerization rates from kymographs of the movie data (Fig. 18A) using cumulative distributions (Fig. 18B) The cumulative distribution data was fit to rising exponential decays to determine the characteristic depolymerization rates (Fig. 18B). The characteristic depolymerization speed is 2.3 ± 0.02 nm/s for wild type katanin p60 on Taxol-stabilized microtubules in the presence of ATP and 1.0 ± 0.009 nm/s with AMPPNP. Clearly, AMPPNP slows the rate of depolymerization. Similar trends are observed for subtilisin microtubules: wild type katanin depolymerizes subtililsin microtubules with a characteristic speed of 1.90 ± 0.07 nm/s in the presence of ATP and 0.78 ± 0.01 nm/s in the presence of AMPPNP.

We also characterized the percent of microtubule ends depolymerized to see if AMPPNP affected the number of microtubule ends depolymerized (Fig. 18D). The data show that 96 ± 2% Taxol-stabilized microtubules are depolymerized in the presence of ATP, while 88 ± 5% are depolymerized in the presence of AMPPNP. These data are likely not statistically significant. Further the percent of subtilisin-treated microtubules depolymerized is not statistically significant when comparing ATP (91 ± 5%) with AMPPNP (92 ± 5%). Thus, neither the presence of the CTT of tubulin nor the presence of AMPPNP affects the number of microtubule ends depolymerized.

Taken together, this data suggests that AMPPNP slows the rate of depolymerization slightly (Fig. 18C), and that is what causes the difference in the total loss of polymer (Fig. 17C). This data further suggests that the presence of ATP is important for end-depolymerization. Further, there is only a minor effect on the depolymerization speed due to the lack of the CTT (Fig. 18C,D). This implies that depolymerization is not just end-severing, but must have a different mechanism that is independent of the CTT.

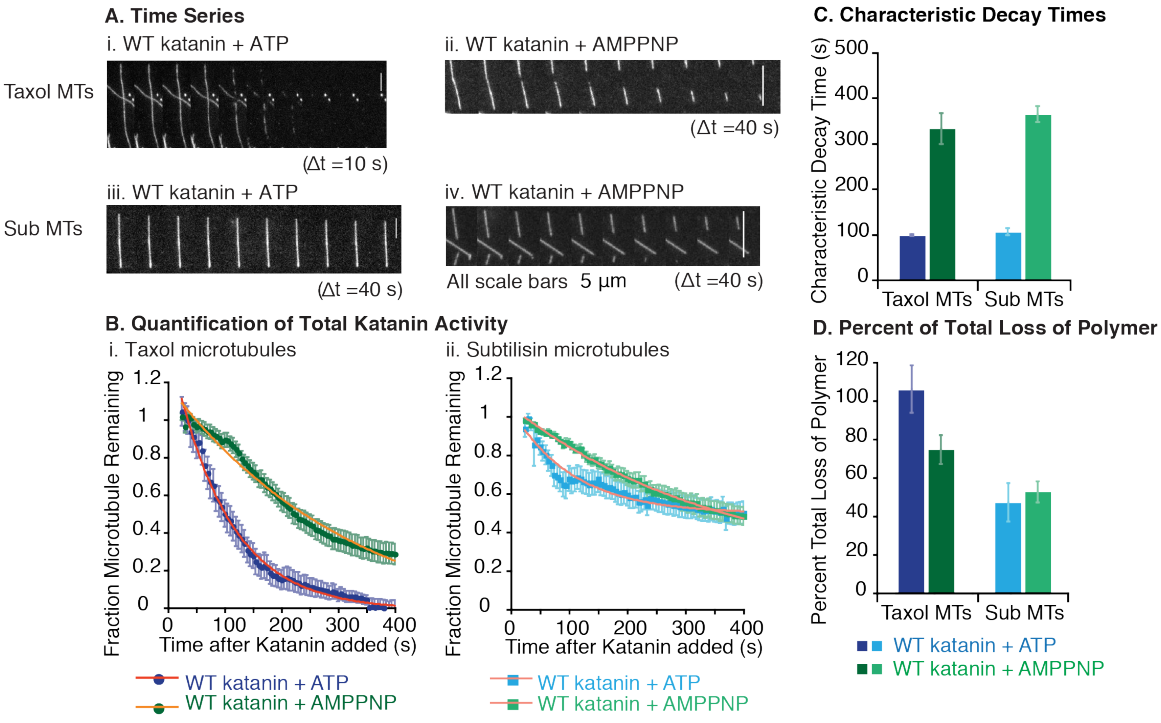

Figure 17. Wild Type Katanin Activity in AMPPNP-bound State.
(A) Time series representative of a severing assay experimental parameters. (i) Taxol microtubules with ATP-bound katanin, and (ii) Taxol microtubules with AMPPNP-bound katanin. (iii) Subtilisin microtubules with ATP-bound katanin and (iv) subtilisin microtubules with AMPPNP-bound katanin. The time between images is as stated below each time series and all the scale bars are all 5 µm. Movies were taken at 5 second intervals for 10 minutes. The first three minutes of each movie was used a control to make sure that the microtubules were stable and not falling apart due to something other than katanin. As shown in Figure 1, katanin was able to sever Taxol microtubules in the presence of ATP. Katanin was also able to sever Taxol microtubules in the presence of the slowly hydrolyzable ATP-analogue, AMPPNP. We observed depolymerization in all conditions. (B) Quantification of loss of polymer for (i) Taxol microtubules and (ii) subtilisin microtubules. Only in chambers with ATP-bound katanin were microtubules completely destroyed during the 10 minutes of the assay. The error bars represent the standard error of the mean. Data was fit with exponential decay parameters for a single exponential (Eq. 3). (i) Taxol microtubules with ATP-bound katanin (dark blue circles, N=66 in 10 different chambers) and (ii) Taxol microtubules AMPPNP-bound katanin (dark green circles, N=47 in 7 different chambers). (iii) Subtilisin microtubules ATP-bound katanin (light blue squares, N=35 in 9 different chambers) and subtilisin microtubules AMPPNP-bound katanin (light green squares, N=33 in 4 different chambers). (C) Quantification of the characteristic decay times (tau) of the exponential decay fits. The characteristic decay times are from the exponential decay fits. The error bars represent the standard error of the mean. (D) Percent total loss of polymer of the different conditions. The error bars are the uncertainty given from the least squares fitting routine.

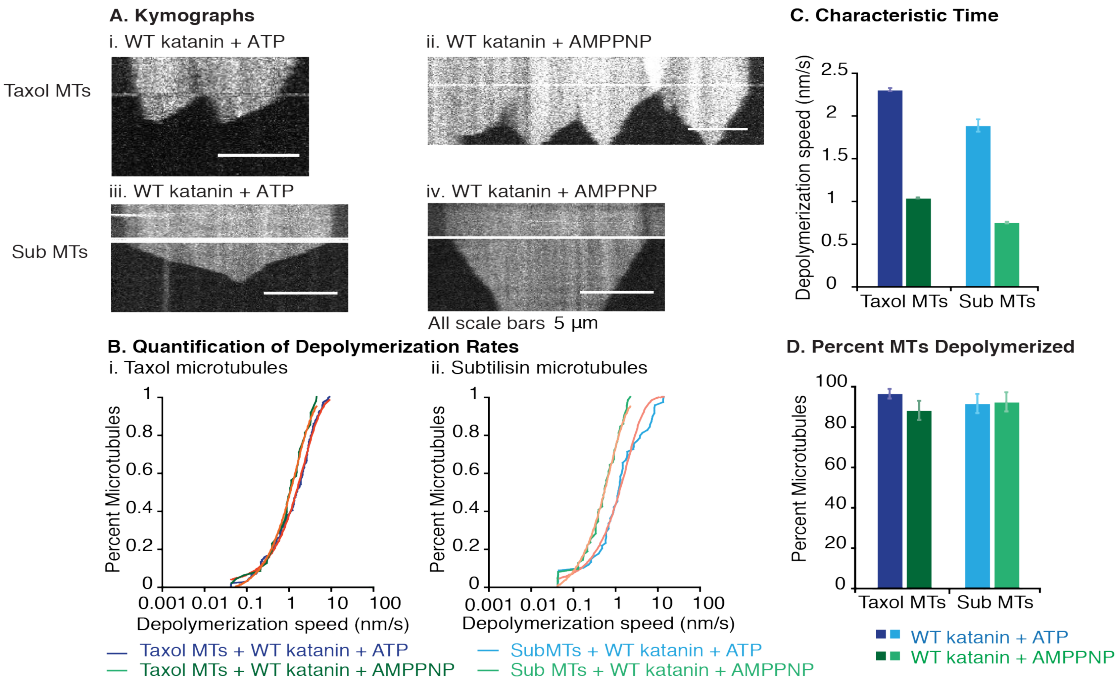

Figure 18. Wild Type Katanin Depolymerization in AMPPNP-bound State.
(A) Kymographs representative of microtubule depolymerization in severing assays. (i) Taxol microtubule with ATP-bound katanin, and (ii) Taxol microtubules with AMPPNP-bound katanin. (iii) Subtilisin microtubules with ATP-bound katanin and, (iv) subtilisin microtubules with AMPPNP-bound katanin. The horizontal white line is when the lights were turned on to flow katanin into the flow chamber. The time is 600 s from the top of the kymograph to the bottom and all the scale bars are 5 µm. Movies were taken at 5 second intervals for 10 minutes. Each pixel is 5 seconds in the x direction and 67.5 nm in the y direction. (B) Cumulative distribution of the depolymerization speeds of (i) Taxol and (ii) subtilisin microtubules with katanin in either the ATP- or AMPPNP-bound state. Taxol microtubules with ATP-bound katanin (dark blue line, N=66 in 10 different chambers) and Taxol microtubules with AMPPNP-bound katanin (dark green line, N=47 in 7 different chambers). Subtilisin microtubules with ATP-bound katanin (light blue line, N=35 in 9 different chambers) and subtilisin microtubules with AMPPNP-bound katanin (light green line, N=33 in 4 different chambers). Data was fit with a rising decay (Eq. 4). (C) Quantification of characteristic depolymerization times for all conditions. The error bars are the error associated with the rising decay time of the fits in (B). (D) Percent of microtubules depolymerized (considered any value above 0.1125 nm/s). This value was determined based on the smallest speed of depolymerization that can be calculated with one pixel wide measurement using the box tool. Error bars represent the standard error of proportion.

3.4 Discussion

Most studies on katanin have focused on its ability to sever microtubules and on elucidating the mechanism of severing. However, depolymerization could be an important mechanism that katanin uses in the cell. For example, katanin is required for proper chromosome segregation during anaphase (Zhang et al., 2007). Katanin stimulates plus-end depolymerization at the kinetochores of spindles, a type of motility termed Pacman (Zhang et al., 2007). It is then thought that other depolymerizing motors like kinesin-13 depolymerize microtubule plus ends to move chromosomes poleward (Rogers et al., 2004). It is possible katanin plays a role after uncapping microtubules by aiding kinesin-13 in actively depolymerizing microtubule plus-ends.

We have shown that depolymerization is a separate activity from severing and that katanin depolymerization and severing have distinct mechanisms. Our evidence for this is 1) depolymerization rates are ATP-dependent; 2) depolymerization rates do not depend on the presence of a CTT whereas severing does; 3) we have evidence that katanin works better as a hexamer than a monomer, but this should be tested further.

The majority of loss of polymer is due to depolymerization in our assays – not severing. We believe severing enables more depolymerization because it allows for more free microtubule ends. The depolymerization rates and the loss of polymer rates are similar for both Taxol microtubules and subtilisin microtubules. However, the amount of polymer lost is lower with subtilisin microtubules, because new ends cannot be made. Such a mechanism might be used in live cells, since severing events would likely trigger catastrophes (depolymerization) of microtubules in cells.

CTTs are not required for depolymerization of microtubules. The negatively charged CTT and the sequence of the CTT is important in regulation of katanin severing. Our assays suggest neither the negatively charged region nor the sequence of the CTT

is important for depolymerization activity. This may have physiological relevance and suggests depolymerization is a more robust mechanism than severing.

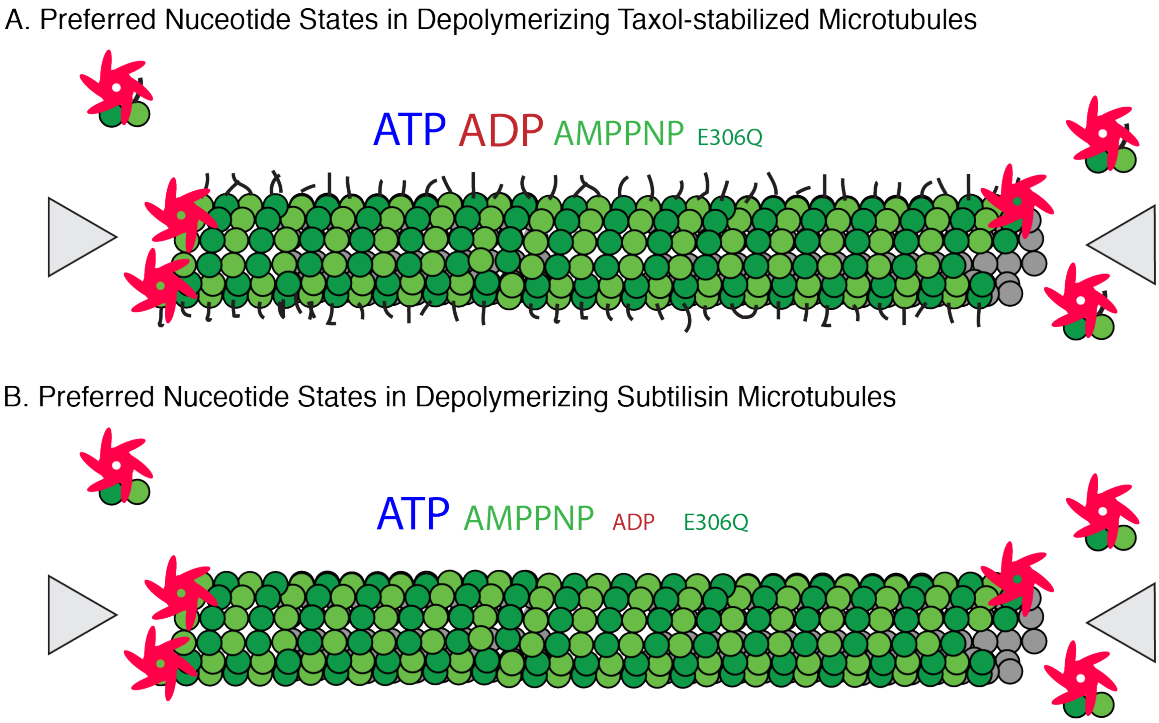

Figure 19. Summary of Preferred Nucleotide States in Katanin Depolymerization of Microtubules.
Preferred nucleotide states in depolymerizing A) Taxol-stabilized microtubules and B) sutilisin microtubules. Based on the data, katanin in the presence of ATP depolymerized microtubules with and without the CTT the best. ADP-bound katanin depolymerized Taxol-stabilized microtubules second best while AMPPNP-bound katanin depolymerized subtilisin microtubules second best. The E306Q mutant katanin in the presence of ATP was the worst at depolymerizing microtubules.

CHAPTER 4

FUTURE OUTLOOK

The studies in this thesis have addressed some of the ways in which katanin regulates microtubule dynamics. We have explored the mechanism of katanin depolymerization on microtubules and identified ways in which it is different from the mechanism of katanin severing. The data presented in Chapter 1 demonstrate that the type of katanin activity, either severing or depolymerization, and the level of activity is regulated by concentration of ATP *in vitro*. The data presented in Chapter 2 show that katanin's mechanism of depolymerization is dependent on the nucleotide present and does not depend on the CTT. Despite the progress made in this thesis, many questions remain unanswered, about both the mechanism of katanin severing and depolymerization.

One question that remains is whether subtilisin microtubules are depolymerized at similar rates from both ends of the microtubule. The data shown in Fig.14A is representative of Taxol-stabilized and subtilisin treated microtubules. However, we did not have polarity marked microtubules in this assay, therefore there is no way to tell which end is the plus end and which is the minus end. However, by grouping the data into the fast end and the slower end, we may be able to identify trends to see if subtilisin microtubules are indeed depolymerized from either end at similar rates.

Our lab continues to be interested in understanding the mechanism of katanin severing in addition to elucidating the mechanism of depolymerization. We have created a fluorescently-labeled CTT construct that is a CTT attached to a fluorescent protein. The protein is made to unfold if tugged upon and therefore will extinguish upon unfolding. This will allow us to test the unfoldase mechanism of katanin severing (Bailey, Jiang, Dima, & Ross, 2016). We also aim to better understand the process of katanin

hexamerization on the CTT. Whether full or partial hexamerization occurs before or after katanin lands on the CTT of tubulin remains unknown. We will test this with fluorescently-labeled construct and others given to us by Dr. Dan Sackett at NIH.

APPENDIX A

Constant Phase			
ATP Concentration	**Average (I)**	**Standard Deviation**	**Time Averaged Over (s)**
28 μM	3.366210263	0.917633831	50.22
100 μM	3.448877821	0.913512218	15.36
500 μM	3.125571429	0.707393459	7.92
1 mM	3.170679021	0.917520699	17.1
2 mM	2.649513309	1.060412608	33.3
5 mM	1.521344622	0.512732128	26.16
10 mM	1.127938021	0.398858062	28.74
20 mM	0.15232578	0.177450655	60.36
2 mM ATP-γ-S	2.949652941	1.266139538	14.22
No Katanin	0.009587052	0.045075332	573.12

Exponential Decay Phase
Fit: $I(t) = Aexp(-t/\tau)$

ATP Concentration	**A**	**τ (s)**	**χ^2**	**R^2**
28 μM	4.9366 ± 0.014734	121.26±0.43978	482.73	0.95118
100 μM	5.1283± 0.006793	111.59±0.16484	47.447	0.99297
500 μM	6.1774± 0.069544	28.725±0.29553	73.266	0.93488
1 mM	5.7904± 0.052638	43.8±0.41887	224.73	0.91307
2 mM	5.7679± 0.019368	46.335±0.13221	25.506	0.98813
5 mM	1.7024± 0.006946	101.96±0.47596	30.883	0.9388
10 mM	1.3789± 0.001731	159.35±0.24817	7.3085	0.98859
20 mM	0.18465±0.000615	210.28±0.98453	0.96298	0.89361
2 mM ATP-γ-S	3.0387±0.0053589	181.08±0.43442	97.967	0.97454

Fit parameters for Constant Phase and Exponential Decay Phase for Katanin on Taxol-stabilized Microtubules. Data in Chapter 1.

Maximum Katanin Bound		
ATP Concentration	**Average**	**Standard Error**
28 μM	3.5308	0.15355
100 μM	3.5292	0.10045
500 μM	3.2224	0.10244
1 mM	3.2413	0.095513
2 mM	2.8289	0.10362
5 mM	1.6198	0.056775
10 mM	1.1726	0.04951
20 mM	0.17975	0.022847
2 mM ATP-γ-S	3.1302	0.1775
No katanin	0.03837	0.005644

Maximum GFP-Katanin Intensity at various concentrations of ATP. Data in Chapter 1.

Exponential decay fit: y=Aexp(-t/τ)+B **Linear fit: y=A(1-(t/τ))**							
Condition	**Fit**	**R**	**R^2**	**χ^2**	**A**	**τ (s)**	**B**
Taxol MTs	Linear Approximation	0.971	0.944	0.00433	0.840 ± 0.002	3224.1 ± 83.226	
Taxol MTs	Exponential decay	0.972	0.944	0.00426	0.482 ± 0.362	1615.4 ± 1400.4	0.361 ± 0.365
Taxol MTs + WT katanin	Exponential Decay	0.997	0.994	0.0413	1.450 ± 0.0172	97.428 ± 2.241	-0.0130 ± 0.00629
Sub MTs	Linear Approximation	0.434	0.189	0.0114	1.107 ± 0.003	22187 ± 5159.8	
Sub MTs + WT katanin	Exponential Decay	0.97217	0.94512	0.05928	0.49536 ± 0.0082946	105.17 ± 7.7913	0.54759 ± 0.019147

Total Loss of Polymer Fits for Wild Type Katanin on Taxol and Subtilisin Microtubules. Data in Chapter 2.

Rising decay fit: y=1-Aexp(-t/τ) **Double rising decay fit: y=1-Aexp(-t/τ)-A_2exp(-t/τ_2)**								
Condition	**Fit**	**R**	**R^2**	**χ^2**	**A**	**τ (s)**	**A_2**	**τ_2 (s)**
Taxol MTs	Rising Decay	0.831	0.690	2.349	0.828 ± 0.0502	0.139 ± 0.0298		
Taxol MTs + WT katanin	Rising Decay	0.998	0.996	0.0577	0.979 ± 0.00351	2.300 ± 0.0178		
Sub MTs	Rising Decay	0.717	0.515	2.345	3.143 ± 2.701	0.0181± 0.00930		
Sub MTs + WT katanin	Rising Decay	0.984	0.969	0.180	0.980 ± 0.0160	1.886 ± 0.0712		
Sub MTs + WT katanin	Rising Double Decay	0.993	0.986	0.0790	0.795 ± 0.0680	1.268 ± 0.128	0.220 ± 0.0713	8.881 ± 3.447

Loss of Polymer Due to Depolymerization Fits for Wild Type Katanin on Taxol and Subtilisin Microtubules. Data in Chapter 2.

Exponential decay fit: y=Aexp(-t/τ)+B							
Condition	**Fit**	**R**	**R^2**	**χ^2**	**A**	**τ (s)**	**B**
Taxol MTs + WT katanin + ADP	Exponential Decay	0.996	0.991	0.0137	0.974 ± 0.0737	556.14 ± 65.676	0.0221± 0.0784
Taxol MTs + E306Q katanin + ATP	Exponential Decay	0.99398	0.98799	0.012465	0.49176 ± 0.020324	284.81 ± 20.675	0.57166 ± 0.016091
Sub MTs + WT katanin +ADP	Exponential Decay	0.993	0.986	0.0132	0.647± 0.0375	408.85 ± 44.38	0.407± 0.0421
Sub MTs + E306Q katanin + ATP	Exponential Decay	0.960	0.921	0.0126	0.206 ± 0.0110	240.19 ± 39.81	0.829 ± 0.0149

Total Loss of Polymer Fits for ADP-bound Katanin and E306Q Mutant Katanin. Data in Chapter 2.

Rising decay fit: y=1-Aexp(-t/τ) **Double rising decay fit: y=1-Aexp(-t/τ)-A_2exp(-t/$τ_2$)**							
Condition	**Fit**	**R**	**R^2**	**$χ^2$**	**A**	**τ (s)**	**A_2**
Taxol MTs + WT katanin + ADP	Rising Decay	0.99785	0.9957	0.057713	0.97935 ± 0.0035058	2.3001 ± 0.017769	
Taxol MTs + E306Q katanin + ATP	Rising Decay	0.958	0.918	0.745	0.870 ± 0.016281	0.430 ± 0.0240	
	Rising Double Decay	0.995	0.989	0.0975	1.144e+08 ± 2.154e+08	0.00221 ± 0.000208	0.695 ± 0.00842
Sub MTs + WT katanin + ADP	Rising Decay	0.99553	0.99109	0.033404	1.0181 ± 0.011223	0.30217 ± 0.0068272	
Sub MTs + E306Q katanin + ATP	Rising Decay	0.97407	0.94881	0.22599	0.88329 ± 0.018764	0.31483 ± 0.018331	

Loss of Polymer Due to Depolymerization Fits for ADP-bound Katanin and E306Q Mutant Katanin. Data in Chapter 2.

Exponential decay fit: y=Aexp(-t/τ)+B							
Condition	**Fit**	**R**	**R^2**	**$χ^2$**	**A**	**τ (s)**	**B**
Taxol MTs + WT katanin + ATP	Exponential Decay	0.997	0.994	0.0413	1.450 ± 0.0172	97.428 ± 2.241	-0.0130 ± 0.00629
Taxol MTs + WT katanin + AMPPNP	Exponential Decay	0.991	0.981	0.0918	1.334 ± 0.0621	332.1 ± 34.277	0.151 ± 0.0740
Sub MTs + WT katanin + ATP	Exponential Decay	0.972	0.945	0.0593	0.548 ± 0.0191	105.17 ± 7.791	0.495 ± 0.00829
Sub MTs + WT katanin + AMPPNP	Exponential Decay	0.998	0.996	0.00702	0.871 ± 0.0210	363.38 ± 17.995	0.180 ± 0.0244

Total Loss of Polymer Fits for Katanin in ATP- and AMPPNP-bound States. Data in Chapter 2.

Rising decay fit: y=1-Aexp(-t/τ) **Double rising decay fit: y=1-Aexp(-t/τ)-A_2exp(-t/$τ_2$)**								
Condition	**Fit**	**R**	**R^2**	**$χ^2$**	**A**	**τ (s)**	**A_2**	**$τ_2$ (s)**
Taxol MTs + WT katanin + ATP	Rising Decay	0.998	0.996	0.0577	0.979 ± 0.00351	2.300 ± 0.0178		
Taxol MTs + WT katanin + AMPPNP	Rising Decay	0.998	0.996	0.0441	1.011 ± 0.00403	1.034 ± 0.00858		
Sub MTs + WT katanin + ATP	Rising Double Decay	0.993	0.986	0.0790	0.795 ± 0.0678	1.268 ± 0.128	0.221 ± 0.0713	8.878 ± 3.444
Sub MTs + WT katanin + AMPPNP	Rising Decay	0.996	0.993	0.0398	1.0542 ± 0.00882	0.748 ± 0.0118		

Loss of Polymer Due to Depolymerization Fits for Katanin in ATP- and AMPPNP-bound States. Data in Chapter 2.

Condition	% Total Loss of Polymer	SE of Proportion	% MT Ends Depolymerized	SE of Proportion
Taxol MTs	13.289	6.8597	30.769	6.281
Taxol MTs + WT katanin	105.74	12.272	96.273	2.332
Taxol MTs + E306Q katanin	36.984	7.3171	57.273	6.090
Taxol MTs + WT katanin + ADP	46.934	10.020	93.75	4.419
Taxol MTs + WT katanin + AMPPNP	74.559	7.4544	88.148	4.715
Sub MTs	3.6700	10.663	10.345	5.560
Sub MTs + WT katanin	47.082	9.9853	91.304	4.763
Sub MTs + E306Q katanin	9.0390	5.7877	54.717	8.665
Sub MTs + WT katanin + ADP	37.552	9.3430	75.56	8.772
Sub MTs + WT katanin + AMPPNP	52.606	5.5367	92.187	4.672
Sub MTs + WT katanin + AMPPNP	52.606	5.5367	92.187	4.672

Percent Total Loss of Polymer and Percent Microtubule Ends Depolymerized in All Conditions. Data in Chapter 2.

APPENDIX B

UVO and Silanization of Coverslips Protocol:

*It is important to clean the racks and glass containers thoroughly before silanization.
*Do not let anything that is not dry come in contact with the silane.
*Rinse container 3X with water then 3X with ddH2O for each step.

UVO Coverslips:

1. Load bent metal coverslip rack with coverslips.
2. UVO for 20 minutes.

Biologically Clean Coverslips:

1. Transfer coverslips from UVO rack to Silane racks.
2. Immerse the coverslips in 100% acetone for 1 hour.
3. Immerse the coverslips in 100% ethanol for 10 minutes.
4. Rinse 3X in ddH2O for 5 minutes each.
5. Immerse the coverslips in 0.1M KOH for 15 minutes (prepare just before use).
6. Rinse 3X in ddH2O for 5 minutes each.
7. Air Dry Coverslips.

Silanization of Coverslips:

1. Once cleaned coverslips have dried completely, immerse in 2% DDS (dimethyldichlorosilane) for 5 minutes.
2. Use a funnel to pour the silane solution back into the bottle to reuse.
3. Immerse the coverslips in 100% ethanol for 5 minutes.
4. Immerse the coverslips in another 100% ethanol for 5 minutes.
5. Rinse 3X in ddH2O for 5 minutes each.
6. Air Dry.

BL21 Cell Transformation for Low Copy Plasmid Protein Purification:

1. Incubate LB/agar plate at 37°C.
2. Dilute DNA to 1 ng/ul in molecular biology water optimize transformation efficiency.
3. Thaw one aliquot of BL21 cells on ice.
4. Once thawed, immediately add 1 ul of diluted DNA to BL21 cells.
5. Leave on ice for 30 min. While cells are incubating with DNA, add 20-30 ul antibiotic to plate. (For high copy plasmids, add 50 ul.)
6. Heat shock at 42°C for EXACTLY 45 sec.
7. Add 250 ul LB/SOC media to cells. Incubate at 37°C for 30 min (incubation optional).
8. Plate 50 ul cell/media mix.

Stbl2 Cell Transformation for Low Copy Plasmid Midiprep:

1. Incubate LB/agar plate at 37C.
2. Dilute DNA to 1 ng/ul in molecular biology water optimize transformation efficiency.
3. Thaw 25 ul of Stbl2 cells on ice.
4. Once thawed, immediately add 1 ul of diluted DNA to Stbl2 cells.
5. Leave on ice for 10 min. While cells are incubating with DNA, add 20-30 ul antibiotic to plate. (For high copy plasmids, add 50 ul.)
6. Heat shock at 42C for EXACTLY 30 sec.
7. Add 250 ul LB/SOC media to 25 ul cells. Incubate at 37C for 30 min.
8. Plate 100 ul cell/media mix.

GenCatch Midiprep for Low Copy Plasmid:

Buffers:
VP1:
50mM Tris-HCl, pH 8.010mM EDTA
Add 100ug/mL RNase A

VP2:
0.2N NaOH
1% SDS

VP3:
3M KoAc, pH 5.5

VPN:
0.1M NaoAc, pH 5.1 * need
1.2M NaCl

VPE:
0.1M Tris-HCl, pH8.5 * pH
1.35M NaCl
15% Isopropanol

1. Put VP3 Buffer on ice before use. Then, transform DNA into DH5a *E. coli* cells, XL10 gold cells, or Stbl2 cells.
2. Culture plasmid-containing bacterial cell in 100 ml of LB medium. Grow no more than 16 hours with vigorous shaking at 37°C.
3. In the morning, harvest the bacterial cells by centrifugation at 6,000 x g for 15 minutes. Rotor: F13S-14x50cy in 50 ml conical tubes.
4. Shake the GenCatchTM Midi column vigorously then equilibrate the column by applying 3 ml of 98% ethanol. Allow the column to be empty by gravity flow and discard the filtrate.
5. Equilibrate the Midi Columns by applying 5-10 ml of VPN Buffer. Allow the column to empty by gravity flow and discard the filtrate.
6. Resuspend the cell pellet in 4 ml of VP1 Buffer. The bacterial cells should be completely resuspended before adding VP2 Buffer.
7. Add 4 ml of VP2 Buffer, mix gently by rotating the lysate and stand for 5 minutes. Do not vortex, vortexing will shear genomic DNA. The lysate should be clear and viscous.
8. Add 4 ml of ice-cold VP3 Buffer, mix gently by rotating. After adding VP3 Buffer, white precipitate should be formed.
9. Centrifuge at 20,000 x g for 15 minutes at 4°C. 20,000 x g corresponds to 12,000 and 13,000 rpm in Beckman JA-17 and Sorvall SS-34 rotors, respectively.
10. Apply the supernatant to the midi column and allow it to flow through by gravity flow and discard the filtrate.
11. Wash the column once with 15 ml of VPN Buffer by gravity flow and discard the filtrate.
12. Apply 5 ml of VPE Buffer to elute DNA by gravity flow.

13. Precipitate DNA by adding 3.75 ml (0.75 volumes) of room temperature isopropanol to the eluate. Mix and centrifuge at 15,000xg for 30 minutes at 4°C. Carefully remove the supernatant.
14. Wash the DNA pellet with 5 ml of room temperature 70% ethanol and centrifuge at 15,000 x g for 10 minutes. Carefully remove the supernatant. Pulse spin and remove remaining ethanol.
15. Dissolve the DNA in 100 µl or a suitable volume of TE or ddH2O.
16. Some insoluble material may also elute out from the column at step 10. To eliminate the insoluble material, load the dissolved DNA sample into a Spin Column (sitting in a 1.5 ml tube) and spin at full speed in a microcentrifuge for 20 seconds, collect the eluted DNA sample in the 1.5 ml tube.
17. Store DNA at -20°C.

Bacterial Katanin Purification Protocol:

Resuspension Buffer:

20 mM Hepes pH 7.7
250 mM NaCl
10% glycerol
*0.5 mM BME
*0.25 mM ATP
*Protease inhibitors:
25uL 2 mg/mL Aprotinin
25uL 2 mg/mL Pepstatin
25uL 2 mg/mL Leupeptin
* Add on Day 4 to 25mL of Resuspension buffer

Katanin Activity Buffer (KAB):

20 mM Hepes pH 7.7
2 mM $MgCl_2$
10 % glycerol

Day 1:

1. Incubate LB/carbenicillin plate upside down at 37°C.
2. Thaw BL21 cells and pMAL-c2x-MBP-sfGFP-p60 plasmid (dated 7/1/14 MB in DNA stocks box).
3. Immediately add 2µL plasmid and let incubate for 30 minutes on ice.
4. Immediately heat shock the cells for EXACTLY 45 seconds @ 42°C in the water bath then place on ice for 2 minutes.
5. Add 400µL of LB media to the tube & place in the incubator for 1 hour (incubation optional).
6. Plate 100µL of the cells onto LB/carbenicillin plate & spread thoroughly, then place in the 37°C incubator for the night.

Day 2:

1. In the morning, check that colonies have started growing on the plate. If they are abundant, wrap the edge of the plate in parafilm and place in the deli fridge. If they are small, allow them to grow for a few more hours, then do the same.
2. Email someone from Tom's lab to use the incubator tomorrow.
3. Make 1-2 flasks of 400mL LB media for use on day 3 & autoclave
    a. Each LB media consists of 4g Tryptone, 4g NaCl & 2g Yeast Extract
4. In the afternoon, make 1-2 Falcon tubes each containing 5 ml of LB & 5µl of carbenicillin.
5. Pick 3 colonies from the plate (try and take colonies that are not surrounded by satellite colonies and are somewhat secluded) and put them in the Falcon tubes.
6. Put the Falcon tubes in the incubator @ 37°C to shake overnight.

Day 3:

1. In the morning, add 400 µl of carbenicillin to the starter cultures & dump them into the 400 ml LB flasks from yesterday (careful not to dump the pipette tip or toothpick you used to pick the colonies into the larger flask)
2. Allow the flasks to shake in the 37°C incubator until the OD reaches 0.8, this usually takes around 3-4 hours.

3. Add 400 µl IPTG (1 mM final concentration from a 1M stock) to each flask.
4. Shake @ 16°C overnight in incubator in centrifuge room for 15-18 hours (or in Tom Maresca's lab - code is 7995).

Day 4:

1. Gather cells from incubator. Transfer into white capped centrifuge tube.
2. Pellet bacteria at 5,000 rpm for 15 min. DO NOT FREEZE.
3. Make up 25 ml of resuspension buffer.
   *Remember to add Protease inhibitors, ATP, and BME.
4. Resuspend pellets in ~15 ml of Resuspension Buffer.
5. Lyse cells using the sonicator every 20 seconds for 20 seconds for a total of 3 minutes on level 4.
6. Transfer sonicated lysate to small, red capped centrifuge tube.
7. Centrifuge in T865 at 13,000 rpm for 30 minutes.
8. Incubate lysate with ~1 ml bed volume of amylose resin for ~1.5-2 hours at 4°C.
   *Wash resin before in column/resuspension buffer 3x. 2x with water, 1x with resuspension buffer at 3,000 RPM for 5 minutes each.
9. Pour lysate into column and wash with ~20 mL of resuspension buffer.
   * Remember to add ATP and BME to new 25 mL of RB.
10. Elute with 10 mM Maltose in resuspension buffer (50 µl of 1 M maltose to 5ml of completed resuspension buffer).
11. Perform a dot blot to prove most concentrated elution.
12. Perform a Bradford at 600 nm and note concentration.
13. Store protein in 50% glycerol aliquots in -80°C.

Tubulin Purification from Pig Brains Protocol:

Stock Solutions: Buffer (200mL)	PM Buffer (200mL)	PMG
200mM PIPES	100mL	76mL
200mM EGTA	2mL	2mL
100mM $MgSO_4$	2mL	2mL
13.7M Glycerol	-------	116mL

	Super PMG (200mL)
1M PIPES	16mL
1M $MgSO_4$	2mL
200mM EGTA	2mL
13.7M Glycerol	175.2mL

1. Clean brains (3) and put in pre-tared 1L beaker
2. Weigh cleaned brains: _____g
3. Put brains in blender
   Add 0.5mL PM buffer per 1g of brain. Volume of PM: _____mL
4. Pulse blender to homogenize brains
5. Pour blended brains into ultracentrifuge tubes (T865 rotor)
6. Balance tubes
7. centrifuge at 100,000 xg for 45 minutes at 2°C
8. Pour supernatant into 500mL graduated cylinder (use pasteur pipettes to get all sup)
   Volume of sup: _____mL
9. Add same volume of PMG to the sup (1:1 PMG:sup ratio)
   *If sup volume is greater than 100 mL, add ½ volume of sup as super PMG
10. Add GTP to final concentration of 1mM
    _____mL of 100 mM GTP stock
11. Mix by inverting cylinder (cover with parafilm)
12. Put sup into new T865 centrifuge tubes and balance
13. Polymerize MTs for 45 minutes at 37°C in water bath
14. Set ultracentrifuge to 37°C, place T865 rotor in 37°C incubator to warm up
15. Centrifuge at 100,000xg in T865 rotor for 45 minutes at 37°C
    These are the 1X Pellets (can drop freeze and store at -80°C or continue)

2X Pellets:

1. Add PM to pellets using 1/5 volume of original homogenate (step 3)
   Volume of PM Buffer added: _____mL
2. Using a thin, pointed spatula, scrape pellet off side of centrifuge tube and into PM buffer
   Lightly shake tube to make sure pellet is loose
   Quickly dump PM buffer + pellet into 15mL dounce in ice slurry
   Repeat for each pellet
3. Homogenize pellets in cold dounce until no large chunks seen (will be cloudy)
   Incubate on ice 30 minutes and homogenize every 2-3 minutes (avoid excessive bubbling)
4. Put homogenized tubulin into ultra (T865) centrifuge tubes

5. Centrifuge 100,000xg for 30 minutes at 2°C
6. Pour sup into graduated cylinder and approximate volume
   Volume of supernatant: _____mL
7. Add PMG buffer 1:1 with supernatant
   Add _____mL PMG
8. Add GTP to final concentration of 1mM
   Add _____mL 100mM GTP stock
9. Mix by inverting
10. Put supernatant into new ultra T865 centrifuge tubes and incubate 45 minutes at 37°C in water bath
11. Centrifuge at 37°C for 45 minutes at 100,000xg
12. Remove most of sup, leaving a small amount to cover pellets
13. Drop freeze pellets in liquid nitrogen and store at -80°C

<u>High Salt Purification</u>

1. Quickly thaw pellets at 37°C (in water bath), dump excess supernatant that froze with pellet
2. Take 2X pellets (2) and homogenize in 5mL PM buffer for 30 minutes on ice (as in step 3 above)
3. Spin at 100,000xg at 4°C (T865 rotor) for 30 minutes
4. Save sup and add:
   5.5 mL 1M PIPES
   1.2 mL DMSO
   120 uL 100mM GTP
   120 uL 200mM EGTA
   12 uL 1M $MgSO_4$
5. Incubate at 37°C for 10 minutes
6. Spin 20 minutes at 20,000xg at 37°C (T865 rotor)
7. Homogenize pellet in 4 mL PEM-100 on ice for 30 minutes
8. Spin 30 minutes at 100,000xg at 4°C (T865 rotor)
9. Bradford of tubulin
   Dilute to 5 mg/mL using PEM-100
   Drop freeze in liquid nitrogen and store in -80°C

Resuspension of Tubulin for Higher Concentration:

1. Prewarm rotor T865 in the incubator at 37°C. Fill the centrifuge tubes halfway with a glycerol cushion consisting of 60% glycerol in PEM-100. Place these in the rotor and allow them to equilibrate to 37°C. While this is happening, proceed with the polymerization of tubulin.
2. Thaw tubulin rapidly using a waterbath at 37°C until the tube is half full of ice. Continue to thaw the remainder on ice.
3. Add 1mM GTP and polymerize microtubules for 40 minutes at 37°C waterbath.
4. Layer the polymerized tubulin onto the prewarmed cushions using tips with large openings to avoid shearing. Centrifuge at 226,240xg for 60 minutes.
5. Aspirate away the supernatant above the cushion and the cushion. Resuspend the pellet in PEM-100 so that the final concentration of tubulin is between 10-20 mg/ml.
6. Incubate on ice for 15 minutes to depolymerize microtubules.
7. Snap freeze and aliquot. Store in -80°C.

Making Cytoskeleton Taxol Stabilized Microtubules: 11% labeled

Unlabeled Cytoskeleton Tubulin: The stock comes in a pellet that needs 200 uL of PEM-100 added to it to be at 5 mg/mL (on ice). Aliquot and drop freeze from stock. Keep sticker on tube in notebook. Only use unlabeled house tubulin if very clean with no MAPs.

Labeled Cytoskeleton Tubulin: Add 4 uL PEM-100 to resuspend pellet to 5 mg/mL before use. Keep sticker on tube in notebook.

1. Turn on large Sorvall Discovery M120 centrifuge, set to 4°C. Make sure vacuum is on.
2. Thaw/resuspend tubulin on ice. Transfer:
   2 uL labeled + 16 uL unlabeled = 18 uL Total
   into open round-bottom centrifuge tubes. (Make balance of same volume!)
3. Incubate on ice for 10 min.
4. Using the small S120AT2-0449 rotor in deli fridge, centrifuge @ 90,000 rpm (366,000xg) for 10 min. Thaw aliquot of 100 mM GTP for next step.
5. Discard pellet & transfer sup to a 1.5 mL epp. tube. Add 0.2 uL 100mM GTP (1mM GTP Final). From this point on <u>DO NOT PUT MICROTUBULES ON ICE.</u>
6. Incubate for 20 min in 37°C water bath.
7. Add 0.2 uL 2mM Taxol (50µM Taxol Final).
8. Incubate for 20 min in 37°C water bath.
9. Using table-top centrifuge 5415 R, centrifuge at 13,200rpm (16,100xg) (top speed) @ 25°C for 10 minutes. (Make a balance of same vol.!)
10. Discard sup & resuspend pellet in:
    0.2 uL 2 mM Taxol + 17.5 uL PEM-100 = 18 uL Total
    *Use same vol. of Taxol as in step 6 and add PEM-100 to the same total vol. in step 2.
11. **Clean 25 uL Hamilton syringe with ddH2O (fill and expel at least 3x). Use syringe to resuspend pellet (fill and expel at least 3x - try not to introduce bubbles).**
12. Incubate overnight in 37°C water bath (~1 night max) after keep at room temp (if too cold keep in incubator).
13. **Use pipette to declump again before use.**

Assay Protocols:

Severing Assay ATPase

* Chambers are assembled on glass slides that have been washed with 70% ethanol. Use double stick tape to make a chamber with a UVO & silanized coverslip.

1. Flow in 2% anti-tubulin antibody (0.4 µL YL1/2 MAB 1864 tubulin antibody + 9.6 µL PEM-100.
   Incubate 5 minutes.
2. Flow in 5% F-127 in PEM-100. Incubate for 5 minutes.
3. Flow in 1:100 MTs in PEM-100. Incubate 5-7 minutes.
4. Flow in KAB-rxn #1 buffer.
5. Image 3 minutes.
6. Flow in Katanin in KAB-rxn buffer #2 (1:10 katanin:rxn buffer).

10x katanin solution:

2.5 µL	Maltose (1µM in KAB)
1 µL	DTT (1 M stock)
__ µL	KRB
__ µL	katanin

50 µL TOTAL

10x free tubulin solution:

__ µL	Unlabeled tubulin (5 mg/mL)
__ µL	BSA (10 mg/mL in KAB)

__ µL TOTAL

For (0 added) 28µM ATP:

KAB-rxn Buffer 1:

2 µL	5% F-127
1 µL	DTT (1 M stock)
1 µL	BSA (100 mg/mL stock)
0.5 µL	Taxol (2 mM stock)
0 µL	ATP
1 µL	glucose (300 mg/mL stock)
1 µL	deoxy
13.5 µL	KAB

20 µL TOTAL

KAB-rxn Buffer 2:

2 µL	5% F-127
1 µL	DTT (1 M stock)
1 µL	BSA (100 mg/mL stock)
0.5 µL	Taxol (2 mM stock)
0 µL	ATP
1 µL	glucose (300 mg/mL stock)
1 µL	deoxy
2 µL	Katanin (10x stock)
11.5 µL	KAB

20 µL TOTAL

For 100µM ATP:

KAB-rxn Buffer 1:

2 µL	5% F-127
1 µL	DTT (1 M stock)
1 µL	BSA (100 mg/mL stock)
0.5 µL	Taxol (2 mM stock)
1.0 µL	ATP (2 mM stock)
1 µL	glucose (300 mg/mL stock)
1 µL	deoxy
12.5 µL	KAB

20 µL TOTAL

KAB-rxn Buffer 2:

2 µL	5% F-127
1 µL	DTT (1 M stock)
1 µL	BSA (100 mg/mL stock)
0.5 µL	Taxol (2 mM stock)
1.0 µL	ATP (2 mM stock)
1 µL	glucose (300 mg/mL stock)
1 µL	deoxy
2 µL	Katanin (10x stock)
10.5 µL	KAB

20 µL TOTAL

For 500µM ATP:

KAB-rxn Buffer 1:

2 µL	5% F-127
1 µL	DTT (1 M stock)
1 µL	BSA (100 mg/mL stock)
0.5 µL	Taxol (2 mM stock)
1.0 µL	ATP (10 mM stock)
1 µL	glucose (300 mg/mL stock)
1 µL	deoxy
12.5 µL	KAB

20 µL TOTAL

KAB-rxn Buffer 2:

2 µL	5% F-127
1 µL	DTT (1 M stock)
1 µL	BSA (100 mg/mL stock)
0.5 µL	Taxol (2 mM stock)
1.0 µL	ATP (10 mM stock)
1 µL	glucose (300 mg/mL stock)
1 µL	deoxy
2 µL	Katanin (10x stock)
10.5 µL	KAB

20 µL TOTAL

For 1mM ATP:

KAB-rxn Buffer 1:

2 µL	5% F-127
1 µL	DTT (1 M stock)
1 µL	BSA (100 mg/mL stock)
0.5 µL	Taxol (2 mM stock)
1.0 µL	ATP (20 mM stock)
1 µL	glucose (300 mg/mL stock)
1 µL	deoxy
12.5 µL	KAB

20 µL TOTAL

KAB-rxn Buffer 2:

2 µL	5% F-127
1 µL	DTT (1 M stock)
1 µL	BSA (100 mg/mL stock)
0.5 µL	Taxol (2 mM stock)
1.0 µL	ATP (20 mM stock)
1 µL	glucose (300 mg/mL stock)
1 µL	deoxy
2 µL	Katanin (10x stock)
10.5 µL	KAB

20 µL TOTAL

For 2mM ATP:

KAB-rxn Buffer 1:

2 µL	5% F-127
1 µL	DTT (1 M stock)
1 µL	BSA (100 mg/mL stock)
0.5 µL	Taxol (2 mM stock)
1.0 µL	ATP (40 mM stock)
1 µL	glucose (300 mg/mL stock)
1 µL	deoxy
12.5 µL	KAB

20 µL TOTAL

KAB-rxn Buffer 2:

2 µL	5% F-127
1 µL	DTT (1 M stock)
1 µL	BSA (100 mg/mL stock)
0.5 µL	Taxol (2 mM stock)
1.0 µL	ATP (40 mM stock)
1 µL	glucose (300 mg/mL stock)
1 µL	deoxy
2 µL	Katanin (10x stock)
10.5 µL	KAB

20 µL TOTAL

For 5mM ATP:

KAB-rxn Buffer 1:

2 µL	5% F-127
1 µL	DTT (1 M stock)
1 µL	BSA (100 mg/mL stock)
0.5 µL	Taxol (2 mM stock)
1.0 µL	ATP (100 mM stock)
1 µL	glucose (300 mg/mL stock)
1 µL	deoxy
12.5 µL	KAB

20 µL TOTAL

KAB-rxn Buffer 2:

2 µL	5% F-127
1 µL	DTT (1 M stock)
1 µL	BSA (100 mg/mL stock)
0.5 µL	Taxol (2 mM stock)
1.0 µL	ATP (100 mM stock)
1 µL	glucose (300 mg/mL stock)
1 µL	deoxy
2 µL	Katanin (10x stock)
10.5 µL	KAB

20 µL TOTAL

For 10mM ATP:

KAB-rxn Buffer 1:

2 µL	5% F-127
1 µL	DTT (1 M stock)
1 µL	BSA (100 mg/mL stock)
0.5 µL	Taxol (2 mM stock)
2.0 µL	ATP (100 mM stock)
1 µL	glucose (300 mg/mL stock)
1 µL	deoxy
11.5 µL	KAB

20 µL TOTAL

KAB-rxn Buffer 2:

2 µL	5% F-127
1 µL	DTT (1 M stock)
1 µL	BSA (100 mg/mL stock)
0.5 µL	Taxol (2 mM stock)
2.0 µL	ATP (100 mM stock)
1 µL	glucose (300 mg/mL stock)
1 µL	deoxy
2 µL	Katanin (10x stock)
9.5 µL	KAB

20 µL TOTAL

For 20mM ATP:

KAB-rxn Buffer 1:

2 µL	5% F-127
1 µL	DTT (1 M stock)
1 µL	BSA (100 mg/mL stock)
0.5 µL	Taxol (2 mM stock)
4.0 µL	ATP (100 mM stock)
1 µL	glucose (300 mg/mL stock)
1 µL	deoxy
9.5 µL	KAB

20 µL TOTAL

KAB-rxn Buffer 2:

2 µL	5% F-127
1 µL	DTT (1 M stock)
1 µL	BSA (100 mg/mL stock)
0.5 µL	Taxol (2 mM stock)
4.0 µL	ATP (100 mM stock)
1 µL	glucose (300 mg/mL stock)
1 µL	deoxy
2 µL	Katanin (10x stock)
7.5 µL	KAB

20 µL TOTAL

Single molecule katanin binding CTT assay

*Chambers are assembled on glass slides that have been washed with 70% ethanol. Use double stick tape to make a chamber with a silanized coverslip.

1. Flow in 2% anti-BSA antibody (0.4uL 50% glycerol antibody at 1 mg/mL + 9.6 uL KAB). Incubate 5 minutes.
2. Flow in 5% F-127. Incubate 5 minutes.
3. Flow in _____ dilution BSA-CTT-Alexa647. Incubate 5 minutes.
    a. Full strength 8.3µM
    b. 1:10 (830 nM)
    c. 1:100 (83 nM)
    d. 1:1,000 (8.3 nM)
4. Flow in KAB-rxn #1 buffer.
5. Take a picture. Image 5 minutes (no delay) to check single molecules and photobleaching.
    a. Use red laser, four colour TIRF 648 cube for CTT channel. Exposure 300 ms
6. Move to a new spot. Flow in katanin in KAB-rxn #2 buffer.
    a. With ATP-γ-S to trap katanin on the CTT
    b. With ATP
7. Image 5 minutes (no delay) in two channels.
    a. Use red laser, four colour TIRF 648 cube for CTT channel. Exposure 300 ms
    b. Use green laser, GFP TIRF cube for katanin channel. Exposure 30 ms .

KAB-rxn Buffer 1:
2 µL 5% F-127
1 µL DTT (1 M stock)
1 µL BSA (100 mg/mL stock)
1 µL ATP (40 mM stock)
1 µL glucose (300 mg/mL stock)
1 µL deoxy
13 µL KAB
20 µL TOTAL

KAB-rxn Buffer 2:
2 µL 5% F-127
1 µL DTT (1 M stock)
1 µL BSA (100 mg/mL stock)
1 µL ATP-γ-S (40 mM stock)
1 µL glucose (300 mg/mL stock)
1 µL deoxy
2 µL Katanin (10x stock)
11 µL KAB
20 µL TOTAL

KAB-rxn Buffer 2:

2 µL 5% F-127
1 µL DTT (1 M stock)
1 µL BSA (100 mg/mL stock)
1 µL ATP (40 mM stock)
1 µL glucose (300 mg/mL stock)
1 µL deoxy
2 µL Katanin (10x stock)
11 µL KAB
20 µL TOTAL

Analysis Protocols

Single Molecule Photobleaching:

1. Make sure you have version 1.33 or later of ImageJ.
2. Down plugin “Multimeasure”.
3. Open your first time series as a stack of .tif files.
4. Copy your first image of stack and paste into new file of the same width and height.
5. Threshold image so that the background is dark and you select the shoulder of the intensity profile. Click apply.
6. Invert the image if it is not already inverted. If it is, skip this step.
7. Analyze particles. Select a minimum size of 3-5, click show masks and record starts.
8. On mask, dilate ROIs.
9. Watershed ROIs.
10. Open Multimeasure plugin.
11. Click “Add particles” to bring over ROI information on the left menu.
12. Click on your stack.
13. In the left menu, highlight ROIs you want to measure intensity of (skip undesirable ROI blobs).
14. Click the “Multi” button and save results as a .txt file.

Microtubule Intensity Over Time:

1. Open FIJI.
2. Click *file, open* the nd2 file you want to analyze.
3. Click *split channels*, *hyperstack,* and leave all other settings.
    a. Split channels will be: TIRF channel (with katanin, green) and HL647/rhodamine (with MTs, red/purple). The two channels are analyzed in the same way.
2. Click on *image, adjust, brightness/contrast, auto*.
3. **Find the first frame after the lights turn off** and adjust the brightness/contrast if necessary again.
4. Click *plugins, registration, StackReg, translation, OK.* The StackReg function will eliminate microtubule drift.
5. Click on *line tool, segment line*, and trace a microtubule, and double click to set line at the end.
6. Set the measurements you want to analyze. Click *analyze, set measurements*.
7. Click on *plugins, macros, measure stack.*
8. Copy and paste the values into the template excel document as signal for that channel.
9. Mark the microtubule on an image of the first frame only (not your video) with a number by using the Text Tool. Type in the number you wish to label the microtubule and click (simultaneously) *Command* and *D*.
10. Back in your StackReg'ed video, with arrow keys, move the segmented line on the microtubule next to the filament but in the background.
11. Again, click *plugins, macros, measure stack. Control, shift, E* pastes the line to the video so you can measure the same line segment.
12. Copy and paste the measurements into the template excel document as noise for that channel.
13. Repeat steps 4 through 14 for the same microtubule in the other channel (either TIRF or Epi channel, whichever was not done first).

        Repeat steps 7 through 14 for each microtubule in the video.

        It may also be necessary to collect data **before the lights turn on** in the HL647/rhodamine channel. To do so, perform steps 1 through 6 (open the same video again and perform the StackReg function, **this time find the very first frame - only copy and paste data from the first 6 or so frames before the lights turn on**).

14. Calculate the average signal/noise - 1 for each microtubule per frame. There will be no data for when the light is on. To do this, find the average of the values of signal/noise - 1 for the first six frames. Normalize by dividing each value of signal/noise - 1 by this average. Plot intensity on the y axis and frame number on the x axis. Do this for both channels and an exponential decay curve (katanin severing) and an inverted parabola with decay on the end for the second one (katanin binding).

Measure Stack Plugin

```
// Measure Stack
//
// This macro measure all the slices in a stack.

  macro "Measure Stack" {
       saveSettings;
       setOption("Stack position", true);
       for (n=1; n<=nSlices; n++) {
          setSlice(n);
          run("Measure");
      }
      restoreSettings;
  }
```

Fit a Curve and Export Variables in KalediaGraph

* To get accurate tau values, open your video in FIJI and check out the properties to find the frame interval (scroll all the way to the bottom) first. Add a column in Excel that is time (seconds), start at t=0 and add the number of seconds of each frame interval to the one above it.

1. Open Kaleidagraph. Click File, open, select the Excel document of interest. Each tab should appear in a new Kaleidagraph window.
2. Copy and paste Time into column 1 and Fraction of Microtubule Remaining (Signal/Noise - 1) into column 2. Any other averages can go in subsequent columns after column 2.
3. Relabel the boldfaced cells at top of columns before continuing.
4. Highlight ALL cells and click the I for info and select “Float”. This allows Kaleidagraph to read the numbers in the document and up to five decimal places, if you want.
5. You CAN Mask the data in the first few time points before the lights come back on. Highlight the cells, click “Command” and “[“ at the same time. I have found it is better to delete these time points and make t=0 the time when the lights are turned off, for a more accurate tau value.
6. Click Gallery, Linear, Scatter to plot a scatter plot. Select the x value (column 1) and the y value you wish to plot (column 2). Each window will have options to select the data from the columns you want.
7. Curvefit, general, exponential fit (or other fit).
8. Click define and enter the following equation with predicted variables:
   m1*exp(-x/m2)+m3; m1=1; m2=1; m3=0.15; m0=0.2;
9. Select Plot, display equation. Click Function, export all curve fits.

Measuring Depolymerization Speeds in FIJI

1. Open Fiji. *File, open,* select ND2 file or TIF file to open.
2. Click *command + C* to copy the first frame.
3. Click *File, new, image.* Click on the new, black image. Click *command + V* to paste. Click *image, adjust, brightness/contrast*. Click *auto*.
4. Using the text tool, label this with MT number and save labeled image.
5. To make a kymograph, draw a segmented line along the microtubule of the video, make sure to draw slightly past the MT edge, and double click the final point to end the segment.
6. Click on *image, stacks, reslice* (using 1 pixel wide slice). Distance is on the horizontal and time is on the vertical.
7. Save kymograph image with detailed naming system.
8. Click on *analyze, set measurements*, then click *OK*.
9. Click on the rectangular tool.
10. In this data set, there is a brighter horizontal line in the middle of the kymograph, where the lights were turned on and something flown into the chamber. Start from right under the line and click and drag to make a box from the edge of the microtubule at t=0 to t=final.
11. Click on *analyze, measure.*
12. Repeat the process until all desired measurements for the single video are in the measurements box. Save results.
13. Click on the video, click *image, show info.* Record frame interval.
14. Calculate depolymerization speed: where distance (nm) = w

Cumulative Distribution Graph in KaleidaGraph

1. Input data to be sorted into column 1. Label column.
2. Highlight column and select Functions →ascending sort. This will put all the data in order of lowest to highest.
3. In column 2 measure number of items/count. Select Functions →create series → set initial value to 1 and increment to 1 and make sure final value is unclicked → enter. Note the final count number.
4. Bring up the Formula Entry window. Go to windows →formula entry. Make sure any columns are deselected. Set column three equal to column 2 divided by the total number of counts. Enter the formula: c3=c2/#counts, for #counts enter an actual number. Hit run in the Formula Entry window and the Cumulative Distribution results will be tabulated.
    - How to read your results:
        - Column 3 multiplied by 100 is a percentage. Column 1 is in this case depolymerization speed. Therefore, some percent of depolymerization speeds is equal to or less than the column 1 value in that row.
        - Ie. 31% of depolymerization speeds are equal to or less than 0.030037 nm/s.

1. Go to Gallery →Linear →Line. Select the depolymerization speeds/column 1 as X and the cumulative distribution/column 3 as Y. Hit Plot.
2. To fit the curves you may have a Rising Decay or Double Rising Decay. Go to Curve fit →General →Edit General →Rising Decay/Double Rising Decay. Click Define to make sure equations are correct then click OK.
    - Rising Decay equation: 1-m1*exp(-m0/m2);m1=0.5;m2=3
    - Double Rising Decay equation: 1-m1*exp(-m0/m2)-m3*exp(-m0/m4);m1=0.5;m2=3;m3=.5;m4=10
3. Record values in boxes by clicking Curve Fit →Export all Curve Fits.
    - M0=x or depolymerization speed in this case
    - M1=weight of first rising decay
    - M2=time to reach ⅓ the way up the graph; slow ething time
    - M3=weight of second rising decay
    - M4=time to reach ⅓ the way up the graph; fast ething time

Making a Montage with a Scale Bar

1. Select area to be cropped using rectangle tool.
2. Hold shift+x to crop image stack.
3. Click Image, stacks, make montage.
4. For the following, enter these values:
5. columns: 10, rows: 1, first slice: first image after katanin added, last slice: last image, increment: 8 (5 sec between raw images x 8 = delta 40 sec between montage images)
6. Click Analyze, tools, scale bar.
7. Enter these values: Width in microns: 1, Height in pixels: 74 pixels is 5µM (67.5 nm per pixel)

REFEERENCES

Ahmad, F. J., Yu, W., Mcnally, F. J., & Baas, P. W. (1999). An Essential Role for Katanin in Severing Microtubules in the Neuron, *145*(2), 305–315.

Arnal, I., & Wade, R. H. (1995). How does taxol stabilize microtubules? *Current Biology*, *5*(8), 900–908. https://doi.org/10.1016/S0960-9822(95)00180-1

Bailey, M. E., Jiang, N., Dima, R. I., & Ross, J. L. (2016). Invited review: Microtubule severing enzymes couple atpase activity with tubulin GTPase spring loading. *Biopolymers*, *105*(8), 547–556. https://doi.org/10.1002/bip.22842

Bailey, M. E., Sackett, D. L., & Ross, J. L. (2015). Katanin Severing and Binding Microtubules Are Inhibited by Tubulin Carboxy Tails. *Biophysical Journal*, *109*(12), 2546–2561. https://doi.org/10.1016/j.bpj.2015.11.011

Bhattacharyya, B., Sackett, D. L., & Wolff, J. (1985). Tubulin, hybrid dimers, and tubulin S. *Journal of Biological Chemistry*, *260*(18), 10208–10216.

Chen, Y., & Hancock, W. O. (2015). Kinesin-5 is a microtubule polymerase. *Nature Communications*, *6*, 1–10. https://doi.org/10.1038/ncomms9160

Diaz-Valencia, J. D., Morelli, M. M., Bailey, M., Zhang, D., Sharp, D. J., & Ross, J. L. (2011). Drosophila Katanin-60 Depolymerizes and Severs at Microtubule Defects, *100*(May), 2440–2449. https://doi.org/10.1016/j.bpj.2011.03.062

Dixit, R. & Ross, J.L. (2010). Studying Plus-End Tracking at Single Molecule Resolution Using TIRF Microscopy. *Methods in Cell Biology*. 95, 543-554.

Eckert, T., Le, D. T. Van, Link, S., Friedmann, L., & Woehlke, G. (2012). Spastin's Microtubule-Binding Properties and Comparison to Katanin. *PLoS ONE*, *7*(12), 1–16. https://doi.org/10.1371/journal.pone.0050161

Frickey, T., & Lupas, A. N. (2004). Phylogenetic analysis of AAA proteins. *Journal of Structural Biology*, *146*(1–2), 2–10. https://doi.org/10.1016/j.jsb.2003.11.020

Hartman, J. J., & Vale, R. D. (1999). Microtubule Disassembly by ATP-Dependent Oligomerization of the AAA Enzyme Katanin, *286*(October), 782–786.

Hawkins, T. L., Sept, D., Mogessie, B., Straube, A., & Ross, J. L. (2013). Mechanical properties of doubly stabilized microtubule filaments. *Biophysical Journal*, *104*(7), 1517–1528. https://doi.org/10.1016/j.bpj.2013.02.026

Hazan, J., Fonknechten, N., Mavel, D., Paternotte, C., Samson, D., Artiguenave, F., … Weissenbach, J. (1999). Spastin, a new AAA protein, is altered in the most frequent form of autosomal dominant spastic paraplegia. *Nature Genetics*, *23*(3), 296–303. https://doi.org/10.1038/15472

Hu, Wen, Pomp, Oz, Ben-Omran, Tawfeg, Kodani, Andrew, Henke, Katrin, Mochida, Ganeshwaran H., Yu, Timothy W., Woodworth, Mollie B., Walsh, C. A. (2015). Katanin p80 Regulates Human Cortical Development by Limiting Centriole and Cilia Number, *84*(6), 1240–1257. https://doi.org/10.1016/j.neuron.2014.12.017.Katanin

Hyman, A. A., Salser, S., Drechsel, D. N., Unwin, N., & Mitchison, T. J. (1992). Role of GTP hydrolysis in microtubule dynamics: information from a slowly hydrolyzable analogue, GMPCPP. *Molecular Biology of the Cell*, *3*(10), 1155–67. https://doi.org/10.1091/mbc.E12-03-0186

Iosefson, O., Olivares, A. O., Baker, T. A., & Sauer, R. T. (2015). Dissection of axial-pore loop function during unfolding and translocation by a AAA+ proteolytic machine. *Cell Reports*, *12*(6), 1032–1041. https://doi.org/10.1016/j.celrep.2015.07.007

Johjima, A., Noi, K., Nishikori, S., Ogi, H., Esaki, M., & Ogura, T. (2015). Microtubule severing by katanin p60 AAA+ATPase requires the C-terminal acidic tails of both alpha-and beta-tubulins and basic amino acid residues in the AAA+ring pore. *Journal of Biological Chemistry*, *290*(18), 11762–11770. https://doi.org/10.1074/jbc.M114.614768

Kapoor, T. M., Mayer, T. U., Coughlin, M. L., & Mitchison, T. J. (2000). Probing spindle assembly mechanisms with monastrol, a small molecule inhibitor of the mitotic kinesin, Eg5. *Journal of Cell Biology*, *150*(5), 975–988. https://doi.org/10.1083/jcb.150.5.975

Loughlin, R., Heald, R., & Nédélec, F. (2010). A computational model predicts Xenopus meiotic spindle organization. *Journal of Cell Biology*, *191*(7), 1239–1249. https://doi.org/10.1083/jcb.201006076

Loughlin, R., Wilbur, J. D., McNally, F. J., Nédélec, F. J., & Heald, R. (2011). Katanin contributes to interspecies spindle length scaling in xenopus. *Cell*, *147*(6), 1397–1407. https://doi.org/10.1016/j.cell.2011.11.014

Maccioni, R. B., Serrano, L., Avila, J., & Cann, J. R. (1986). Characterization and structural aspects of the enhanced assembly of tubulin after removal of its carboxyl-terminal domain. *European Journal of Biochemistry*, *156*(2), 375–381. https://doi.org/10.1111/j.1432-1033.1986.tb09593.x

Matsuo, M., Shimodaira, T., Kasama, T., Hata, Y., Echigo, A., Okabe, M., … Kishimoto, T. (2013). Katanin p60 contributes to microtubule instability around the midbody and facilitates cytokinesis in rat cells. *PLoS ONE*, *8*(11), 1–15. https://doi.org/10.1371/journal.pone.0080392

Mcnally, F. J., & Thomas, S. (1998). Katanin Is Responsible for the M-Phase Microtubule- severing Activity in Xenopus Eggs, *9*(July), 1847–1861.

McNally, F. J., & Vale, R. D. (1993). Identification of Katanin , an ATPase That Severs and Disassembles Stable M icrotubules, *75*, 419–429.

McNally, K., Berg, E., Cortes, D. B., Hernandez, V., Mains, P. E., & McNally, F. J. (2014). Katanin maintains meiotic metaphase chromosome alignment and spindle structure in vivo and has multiple effects on microtubules in vitro. *Molecular Biology of the Cell*, *25*(7), 1037–49. https://doi.org/10.1091/mbc.E13-12-0764

McNally, K. P., Bazirgan, O. a, & McNally, F. J. (2000). Two domains of p80 katanin regulate microtubule severing and spindle pole targeting by p60 katanin. *Journal of Cell Science*, *113 (Pt 9*, 1623–1633.

Mitchison, T. (1993). Localization of an exchangeable GTP binding site at the plus end of microtubules. *Science*, *261*(5124), 1044–1047. https://doi.org/10.1126/science.8102497

Mitchison, T., & Kirschner, M. (1984). Dynamic instability of microtubule growth. *Nature*, *312*(5991), 237–42. https://doi.org/10.1038/312237a0

Nadar, V. C., Ketschek, A., Myers, K. A., Gallo, G., & Baas, P. W. (2008). Kinesin-5 Is Essential for Growth-Cone Turning. *Current Biology*, *18*(24), 1972–1977. https://doi.org/10.1016/j.cub.2008.11.021

Nogales, E. (1999). A structural view of microtubule dynamics. *Cellular and Molecular Life Sciences*, *56*(1–2), 133–142. https://doi.org/10.1007/s000180050012

Nogales, E., Whittaker, M., Milligan, R. A., & Downing, K. H. (1999). High-resolution model of the microtubule. *Cell*, *96*(1), 79–88. https://doi.org/10.1016/S0092-8674(00)80961-7

Paglini, G., Peris, L., Mascotti, F., Quiroga, S., & Caceres, A. (2000). Tau protein function in axonal formation. *Neurochemical Research*, *25*(1), 37–42. https://doi.org/10.1023/A:1007531230651

Rogers, G. C., Rogers, S. L., Schwimmer, T. A., Ems-McClung, S. C., Walczak, C. E., Vale, R. D., … Sharp, D. J. (2004). Two mitotic kinesins cooperate to drive sister chromatid separation during anaphase. *Nature*, *427*(January), 364–370. https://doi.org/10.1038/nature02246.1.

Rogers, G. C., Rogers, S. L., & Sharp, D. J. (2005). Spindle microtubules in flux. *Journal of Cell Science*, *118*(6), 1105–1116. https://doi.org/10.1242/jcs.02284

Roll-Mecak, A., & McNally, F. J. (2010). Microtubule-severing enzymes. *Current Opinion in Cell Biology*, *22*(1), 96–103. https://doi.org/10.1016/j.ceb.2009.11.001

Roll-Mecak, A., & Vale, R. D. (2006). Making more microtubules by severing: A common theme of noncentrosomal microtubule arrays? *Journal of Cell Biology*, *175*(6), 849–851. https://doi.org/10.1083/jcb.200611149

Roll-Mecak, A., & Vale, R. D. (2008). Structural basis of microtubule severing by the hereditary spastic paraplegia protein spastin. *Nature*, *451*(7176), 363–367. https://doi.org/10.1038/nature06482

Ross, J. L. (2016). Biophysical Perspective The Dark Matter of Biology. *Biophysj*, *111*(5), 909–916. https://doi.org/10.1016/j.bpj.2016.07.037

Ross, J. L., Santangelo, C. D., Makrides, V., & Fygenson, D. K. (2004). Tau induces cooperative Taxol binding to microtubules. *Proceedings of the National Academy of Sciences of the United States of America*, *101*(35), 12910–12915. https://doi.org/10.1073/pnas.0402928101

Serrano, L., Valencia, A., Caballero, R., & Avila, J. (1986). Localization of the high affinity calcium-binding site on tubulin molecule. *Journal of Biological Chemistry*, *261*(15), 7076–7081. https://doi.org/VL - 261

Sharma, N., Bryant, J., Wloga, D., Donaldson, R., Davis, R. C., Jerka-Dziadosz, M., & Gaertig, J. (2007). Katanin regulates dynamics of microtubules and biogenesis of motile cilia. *Journal of Cell Biology*, *178*(6), 1065–1079. https://doi.org/10.1083/jcb.200704021

Sharp, D. J., & Ross, J. L. (2012). Microtubule-severing enzymes at the cutting edge. *Journal of Cell Science*, *125*(11), 2561–2569. https://doi.org/10.1242/jcs.101139

Srayko, M., Buster, D. W., Bazirgan, O. A., Mcnally, F. J., & Mains, P. E. (2000). MEI-1/MEI-2 katanin-like microtubule severing activity is required for Caenorhabditis elegans meiosis. *Genes & Development*, *14*, 1072–1084. https://doi.org/10.1101/gad.14.9.1072

Tanaka, T. U., & Desai, A. (2008). Kinetochore-microtubule interactions: the means to the end. *Current Opinion in Cell Biology*, *20*(1), 53–63. https://doi.org/10.1016/j.ceb.2007.11.005

Tischfield, M. A., Cederquist, G. Y., Gupta, M. L. J., & Engle, E. C. (2012). Phenotypic spectrum of the Tubulin-related Disorders and Functional Implications of Disease-causing Mutations, *21*(3), 286–294. https://doi.org/10.1016/j.gde.2011.01.003.Phenotypic

Vale, R. D. (1991). Severing of Stable Microtubules by a Mitotically Activated Protein in Xenopus Egg Extracts, *64*, 827–839.

Valenstein, M. L., & Roll-Mecak, A. (2016). Graded Control of Microtubule Severing by Tubulin Glutamylation. *Cell*, *164*(5), 911–921. https://doi.org/10.1016/j.cell.2016.01.019

White, S. R., Evans, K. J., Lary, J., Cole, J. L., & Lauring, B. (2007). Recognition of C-terminal amino acids in tubulin by pore loops in Spastin is important for microtubule severing. *Journal of Cell Biology*, *176*(7), 995–1005. https://doi.org/10.1083/jcb.200610072

Whitehead, E., Heald, R., & Wilbur, J. D. (2013). N-terminal Phosphophorylation of p60 Katanin Directly Regulates Microtubule Severing. *J. Mol Biol.*, *425*(2), 214–221. https://doi.org/10.1126/scisignal.2001449.Engineering

Ye, A. A., & Maresca, T. J. (2015). It's all relative: Centromere- versus pole-based error correction. *Cell Cycle*, *14*(24), 3777–3778. https://doi.org/10.1080/15384101.2015.1105701

Zehr, E., Szyk, A., Piszczek, G., Szczesna, E., Zuo, X., & Roll-mecak, A. (2017). Katanin spiral and ring structures shed light on power stroke for microtubule severing. *Nature Publishing Group*, (August). https://doi.org/10.1038/nsmb.3448

Zhang, D., Grode, K. D., Stewman, S. F., Diaz-valencia, J. D., Liebling, E., Rath, U., … Sharp, D. J. (2011). Drosophila katanin is a microtubule depolymerase that regulates cortical-microtubule plus-end interactions and cell migration, *13*(4). https://doi.org/10.1038/ncb2206

Zhang, D., Rogers, G. C., Buster, D. W., & Sharp, D. J. (2007). Three microtubule severing enzymes contribute to the "Pacman-fl ux" machinery that moves chromosomes. *J. Cell Biol.*, *177*(2), 231–242. https://doi.org/10.1083/jcb.200612011